

RADIOPURITY MEASUREMENT OF ACRYLIC
FOR THE DEAP-3600 DARK MATTER EXPERIMENT

by

CORINA MICHELLE NANTAIS

A thesis submitted to the
Department of Physics, Engineering Physics & Astronomy
in conformity with the requirements for
the degree of Master of Science

Queen's University
Kingston, Ontario, Canada

January 2014

Copyright © Corina Michelle Nantais, 2014

Abstract

The liquid argon target of the DEAP-3600 dark matter detector is contained by an extremely radiopure acrylic vessel. Alpha decays from the inner surface of the acrylic vessel are a source of background. If a fraction of the alpha energy is observed, or if the recoiling nucleus from the alpha decay is observed, the event will not be separated from a dark matter candidate event. In addition to the low level of inherent contamination from uranium and thorium, the ^{210}Pb from ^{222}Rn diffusion during manufacturing must be measured. The limit for the DEAP-3600 acrylic vessel is $1.1 \times 10^{-20} \text{ g/g } ^{210}\text{Pb}$. By vaporizing a large quantity of acrylic and counting the concentrated residue with an ultralow background HPGe well detector and a low background alpha spectrometer, the bulk acrylic was found to have an upper limit of $10^{-19} \text{ g/g } ^{210}\text{Pb}$. The design, installation, commissioning, operation, and analysis for various aspects of the acrylic assay are described.

Acknowledgments

I'd like to thank the following people: my supervisor, Mark Boulay, for his contagious enthusiasm for DEAP and for sending me to many conferences to advertise; Chris Jillings, for his encouragement; Bruce Cleveland, for his patience in listening to me think out loud; Lina Anselmo, for being so kind and always cleaning up after me; Fraser Duncan for buying me a hot dog roller and letting it takeover a fume hood; Brian Morissette and his team, for not letting me build a sloppy, crooked, and duct tape covered, acrylic vaporization system; Eric Vázquez-Jáuregui for always being willing to help with programming when I had no idea what I was trying to do, but somehow he did; Wolfgang Rau, for being free to talk things over at any time; Mark Ward, for so many odds and ends; my officemates; and everyone at Queen's. I have to thank my SNOLAB friends, the locals and the visitors, for making Sudbury fun. Finally, I am so grateful for my family. Most of all I thank Brian, my darling.

Table of Contents

Abstract	i
Acknowledgments	ii
Table of Contents	iii
List of Tables	v
List of Figures	vi
1 Introduction	1
1.1 Evidence for dark matter	1
1.2 Direct detection	2
2 The DEAP experiment	7
2.1 The project	8
2.2 SNOLAB as host	9
2.3 DEAP-3600	9
3 Backgrounds	12
3.1 Classes of backgrounds	12
3.2 Requirements for the Acrylic Vessel	16
3.3 Assay techniques	18
4 The acrylic vaporization system	23
4.1 Vaporization	24
4.1.1 Procedure	24
4.1.2 Commissioning	30
4.1.3 Safety	34
4.2 Acid rinse	35
5 Gamma spectrometry	40

5.1	Performance	41
5.2	Background	42
5.3	Detection efficiency	44
6	Alpha spectrometry	47
6.1	^{210}Po collection	47
6.2	Low background alpha counter	53
6.3	Energy calibration and resolution	54
6.4	Background	56
6.5	Counting efficiency	59
7	Recovery efficiency	61
7.1	^{210}Pb from ^{222}Rn source	61
7.1.1	Successful spike	63
7.1.2	Lucas cell counting	68
7.1.3	Previous attempts	73
7.2	Stable lead from Pb standard	82
8	Results	85
8.1	Blanks	85
8.2	Recovery efficiency	87
8.3	DEAP-3600 acrylic vessel	90
9	Conclusion	95
	Bibliography	97

List of Tables

3.1	Limits in bulk acrylic	18
6.1	Energy calibration and resolution of alpha counters using ^{241}Am . . .	54
7.1	Half-lives for decay of ^{222}Rn to ^{210}Pb	63
7.2	Half-lives for decay of ^{210}Pb to ^{210}Po	63
7.3	Lucas cell ^{222}Rn results from spike	68
7.4	Stable lead spiked samples analyzed by ICP-MS	84
8.1	Blanks in well detector	86

List of Figures

1.1	Current results for spin independent WIMP-nucleon cross section . . .	6
2.1	DEAP-3600 detector	11
3.1	^{238}U decay chain	14
3.2	^{232}Th decay chain	15
4.1	Acrylic vaporization system on surface at SNOLAB	25
4.2	Acrylic vaporization system schematic	26
4.3	Acrylic block before start of vaporization	27
4.4	Observations of acrylic during vaporization	27
4.5	Char removed by adding air to the vaporization furnace	29
4.6	Acid rinses remove residue from boat	37
5.1	Example of ^{210}Pb in well detector	42
5.2	Background of well detector	43
5.3	^{238}U calibration source in well detector	45
5.4	^{232}Th calibration source in well detector	46
6.1	Energy calibration and resolution of alpha counters	55
6.2	Effect of alpha counter dead layer	56
6.3	Background of alpha counters	57
6.4	^{232}Th daughters in alpha counters	58
6.5	Sample and alpha counter solid angle	60
7.1	Lead spike to measure recovery efficiency	64
7.2	Lucas cell counters	70
7.3	Alphas in Lucas cell after spike	71
7.4	Difference between Lucas cell counters	72
7.5	Previous design of lead spike to measure recovery efficiency	74
8.1	Recovery efficiency from well detector	87
8.2	Recovery efficiency from alpha counter	89
8.3	DEAP-3600 AV acrylic ^{210}Pb in well detector	92

8.4 DEAP-3600 AV acrylic ^{210}Pb in alpha counter	93
---	----

Chapter 1

Introduction

It has been established that most of our Universe is not made up of ordinary matter. Although revealed by its gravitational effects, dark matter remains mysterious. Observations of galaxies and galaxy clusters provide evidence for the amount and location of dark matter, as well as how dark matter interacts. A direct detection of the particle is required to investigate its properties. The search for dark matter is an intense global effort, engaging many experiments and a variety of techniques. The direct detection of dark matter would be a major discovery.

1.1 Evidence for dark matter

A brief history of the astrophysical evidence for dark matter is presented. It was Fritz Zwicky, in 1933, who first gave the name ‘dark matter’ to matter that could not be observed [1, 2]. While studying the Coma cluster, he estimated the mass of the galaxy cluster from the amount of light. However, the velocities of the galaxies were greater than could be explained by his estimate of the mass. He concluded that,

in addition to the luminous matter, there must be non-luminous matter. Beginning in 1970, Vera Rubin's measurements of rotation curves indicated that dark matter forms a halo which extends far beyond the luminous matter in a spiral galaxy [3]. The mass estimated from the amount of light could not account for the unexpectedly high velocities of stars measured at large distances from the centre of the galaxy. Gravitational lensing confirms the findings from rotation curves. The mass of a galaxy, or a galaxy cluster, can be determined by observing how light from background galaxies is affected. The amount and location of mass dictates how the images will be distorted. In addition to the amount and location of dark matter, collisions of galaxy clusters also provide information on the nature of dark matter. Dark matter does not interact with baryonic matter, and rarely interacts with itself. The Bullet Cluster, which is the collision of two galaxy clusters, is a popular example [4]. Measurements of the cosmic microwave background (CMB) suggest that the energy density of the Universe is 5% baryonic matter, 27% dark matter, and 68% dark energy [5]. The evidence for dark matter suggests a particle that is neutral, stable, non-relativistic, and non-baryonic. A direct detection of the dark matter particle must be made. The favoured dark matter candidate is the Weakly Interacting Massive Particle (WIMP). Because a WIMP rarely interacts, detection is very challenging.

1.2 Direct detection

Direct detection experiments are designed to measure a WIMP interaction inside of a detector. Energy can be transferred from the WIMP to normal matter through scattering. The transferred energy can be measured as ionization, scintillation, or

phonons, for example. Detectors include solid scintillators, cryogenic solid state detectors, liquid noble gases, and superheated liquids. No matter the technique, a good experiment requires a low energy threshold, low background, and a large target or exposure time to accommodate this rare event search. Select examples of direct detection experiments are discussed.

A well known use of solid scintillators is the DAMA experiment. DAMA/LIBRA, located in the Laboratori Nazionali del Gran Sasso in Italy, reports a 9σ annual modulation over 13 years with NaI(Tl) [6]. This claim has yet to be confirmed, and is inconsistent with exclusion limits from other experiments. ANAIS will attempt to reproduce the results with a detector in the Laboratorio Subterráneo de Canfranc in Spain [7]. At the South Pole, DM-Ice will also attempt to replicate the DAMA experiment [8]. While the dark matter signal would be the same, if the signal is instead due to seasonal effects the modulation will be opposite in the Southern Hemisphere compared to the Northern Hemisphere. Using CsI(Tl), KIMS at the Yangyang Underground Laboratory in Korea concluded that the DAMA signal could not be due to WIMP scattering off of iodine [9].

Cryogenic solid state detectors are widely used. Some experiments make use of both phonons and ionization from an event. CDMS has used germanium and silicon in detectors at the Soudan Underground Laboratory in Minnesota, USA. In germanium, CDMS II published a competitive exclusion limit [10], and a reanalysis with a lower threshold improved the limit for a low mass WIMP [11]. In silicon, however, CDMS II found an excess of events and published an allowed region [12]. The next detector, SuperCDMS, is under development and will be located at SNOLAB near Sudbury, Ontario, Canada. Also with germanium, EDELWEISS-II produced a

limit after running at the Laboratoire Souterrain de Modane (LSM) in France [13]. Instead of ionization, CRESST makes use of phonons and scintillation. CRESST-II at Gran Sasso reported a 4σ signal when the expected background did not account for the number of events observed in CaWO_4 [14]. Collaborators from EDELWEISS and CRESST are continuing with EURECA at LSM. Using only an ionization signal in germanium, CoGeNT found an excess of events during operation at Soudan [15].

A scintillation signal is provided by liquid noble detectors. DEAP, and its use of liquid argon, will be discussed in the next chapter. MiniCLEAN is currently under construction at SNOLAB [16]. The detector will use liquid argon, and possibly liquid neon as well. XMASS, at the Kamioka Observatory in Japan, will use liquid xenon [17]. Other experiments combine both scintillation from the liquid phase, and ionization from drifting the electrons to a gas phase to observe the electroluminescence. There are several two-phase xenon detectors. The LUX result, a spin independent WIMP-nucleon cross section of $<7.6 \times 10^{-46} \text{ cm}^2$ for a 33 GeV WIMP, is the current best limit [18]. LUX is located in the Sanford Underground Research Facility (SURF) in South Dakota, USA. The ZEPLIN experiment, at the Boulby Underground Laboratory in the UK, is coming to an end after presenting its last results from ZEPLIN-III [19]. LUX and ZEPLIN have formed the LZ Collaboration for the next detector. XENON1T is under construction at Gran Sasso after the success of XENON100 [20]. Two-phase argon detectors are another option. ArDM operated a prototype on surface [21], and WARP at Gran Sasso produced an exclusion curve from a prototype detector [22]. Currently, the DarkSide Collaboration is investigating two-phase argon detectors and has been operating the DarkSide-10 prototype at Gran Sasso [23].

Superheated liquids result in a visual, and also acoustic signal, when there is a phase transition. Both at SNOLAB, PICASSO uses the fluorine target in C_4F_{10} [24] and COUPP uses both fluorine and iodine from CF_3I [25]. The PICASSO and COUPP collaborations have merged to form PiCo. SIMPLE uses C_2ClF_5 and is located at the Laboratoire Souterrain à Bas Bruit in France [26].

Lastly, directional detection experiments use reconstructed tracks to identify WIMPs as Earth passes through the dark matter halo around the Milky Way. DRIFT has used CS_2 - CF_4 gas in DRIFT-IIId at Boulby [27]. DMTPC uses CF_4 gas and has been operated on surface [28]. MIMAC will also use CF_4 [29].

This summary, while organizing the major experiments into different detection techniques, has not covered all of the techniques in use. For example, DAMIC uses charge-coupled devices (CCDs) and is now located at SNOLAB [30].

Dark matter sensitivity is presented as a measure of the WIMP-nucleon cross section. There are some standard assumptions, such as the local WIMP density and the WIMP velocity. Nuclei with a net spin are sensitive to the spin of the WIMP, and therefore report spin dependent cross sections. Otherwise, a spin independent cross section is reported. See Figure 1.1 for the current results of the spin independent WIMP-nucleon cross section.

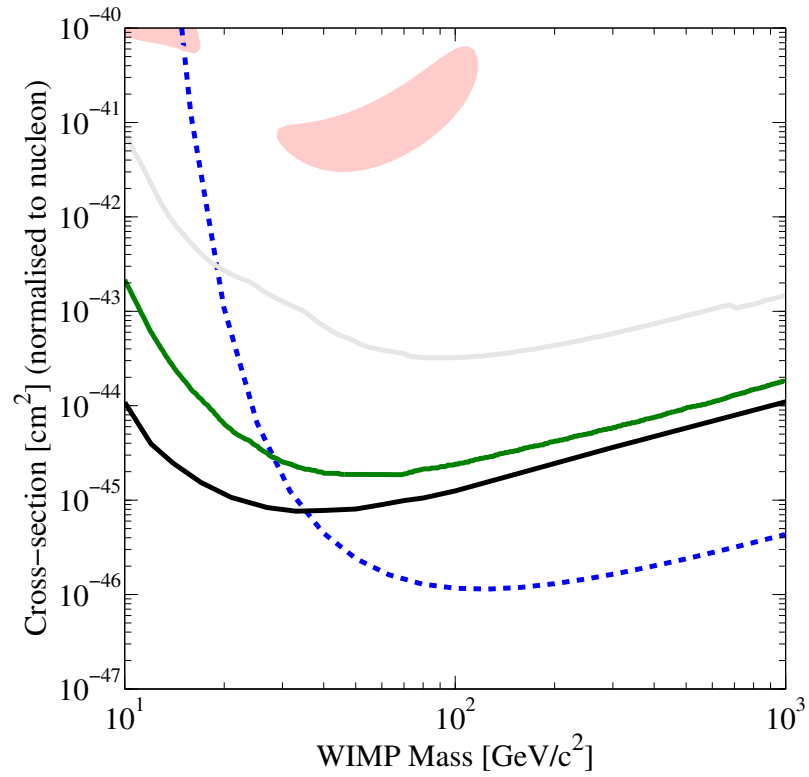


Figure 1.1: Some current results for the spin independent WIMP-nucleon cross section are shown, namely CDMS-EDELWEISS 2011 (grey), XENON100 2012 (green), and LUX 2013 (black), along with the projected limit for DEAP-3600 (blue). Each of these limits excludes the region above. The shaded regions show the area of phase space favoured by DAMA/LIBRA 2008 [31].

Chapter 2

The DEAP experiment

DEAP is an experiment for direct dark matter particle detection using liquid argon scintillation. Argon provides excellent pulse-shape discrimination (PSD) between electromagnetic interactions and nuclear recoils based on scintillation time [32]. After an interaction with a particle, argon atoms become excited and form dimers which can be in either singlet or triplet states. Upon decaying to the ground state, 128 nm photons are emitted. The lifetimes are different: 6 ns for the singlet state and 1.6 μ s for the triplet state. The ratio of the number of singlet states to triplet states depends on the type of particle that caused the excitation [33]. Electromagnetic interactions tend to produce more triplet states, whereas nuclear recoils tend to produce more singlet states. DEAP (Dark matter Experiment with Argon PSD) has developed a technique for separating background events from WIMP candidate events.

2.1 The project

DEAP has developed over the past decade into a competitive dark matter search. Beginning in 2004, simulations and first experiments were performed at Los Alamos National Laboratory. A prototype, DEAP-1, was constructed at Queen's University in 2005, and collected data during 2006–2007. Operation of DEAP-1 continued at SNOLAB during 2007–2012. Meanwhile the successor, DEAP-3600, was designed. DEAP-3600 is under construction at SNOLAB and operation is expected in 2014. There may be motivation for a larger liquid argon detector, on the order of 100 tonnes, depending on the results of the current dark matter experiments. The DEAP collaboration now consists of over 60 researchers from the University of Alberta, Carleton University, Laurentian University, Queen's University, Royal Holloway University of London, Rutherford Appleton Laboratory, SNOLAB, the University of Sussex, and TRIUMF.

The cylindrical DEAP-1 detector, which contained 7 kg of liquid argon and two PMTs, was an invaluable tool. First of all, DEAP-1 demonstrated the PSD technique [34]. Simulations of light production and collection were verified, and fabrication and operation were investigated. Perhaps most importantly, DEAP-1 allowed for a study of backgrounds and background mitigation [35].

DEAP-3600 will contain 3600 kg of liquid argon in an acrylic vessel (AV) surrounded by 255 PMTs. The projected sensitivity to the spin independent WIMP-nucleon cross section of 10^{-46} cm² for a 100 GeV WIMP considers a 15 keV_{ee} (60 keV_r) threshold, a fiducial volume of the inner 1000 kg, and <1 background event in 3 years of livetime [36]. DEAP-3600 is anticipated to be the most sensitive dark matter experiment, and has the potential to detect dark matter.

2.2 SNOLAB as host

SNOLAB achieves the low background necessary for such a sensitive experiment. The 6800 ft level of the Vale Creighton Mine in Sudbury, Ontario, Canada provides approximately 6000 metres water equivalent of shielding from cosmic rays. The entire laboratory operates as a CLASS 2000 cleanroom, and personnel entering the laboratory must shower and change into cleanroom uniforms. The radioactive decays in the surrounding rock can be shielded with various materials, such as water or plastics. Following the success of the Sudbury Neutrino Observatory (SNO), the underground laboratory was expanded to approximately 5000 m². The experimental program also expanded to dark matter and neutrino physics, including low energy solar neutrinos, supernova neutrinos, geoneutrinos, neutrinos from nuclear reactors, and neutrinoless double beta decay. DEAP-3600 is housed in the Cube Hall.

2.3 DEAP-3600

The DEAP-3600 detector is shown in Figure 2.1. The acrylic vessel (AV), with a radius of 85 cm, contains 3600 kg of liquid argon. The inner 55 cm radius sphere, corresponding to 1000 kg of liquid argon, is the fiducial volume. For detection by the 8 inch Hamamatsu R5912 high quantum efficiency PMTs, the 128 nm scintillation photons are shifted to approximately 420 nm by 1,1,4,4-tetraphenyl-1,3-butadiene (TPB). A deposition source has been designed to coat the approximately 10 m² inner surface of the AV with 1 μ m of TPB. Acrylic light guides, 8 inches in diameter and 50 cm long, connect the AV and PMTs. The 50 cm length was set by the requirement to shield from neutrons from the PMTs. The space between the light guides is filled

with high density polyethylene and polystyrene for neutron shielding, and also for thermal insulation. The liquid argon is -190°C and the PMTs are operated at approximately -30°C . The entire detector is contained in the steel shell, and the steel shell is surrounded by the 8 m diameter water shield tank. As a muon veto 48 8 inch Hamamatsu R1408 PMTs face outward from the steel shell.

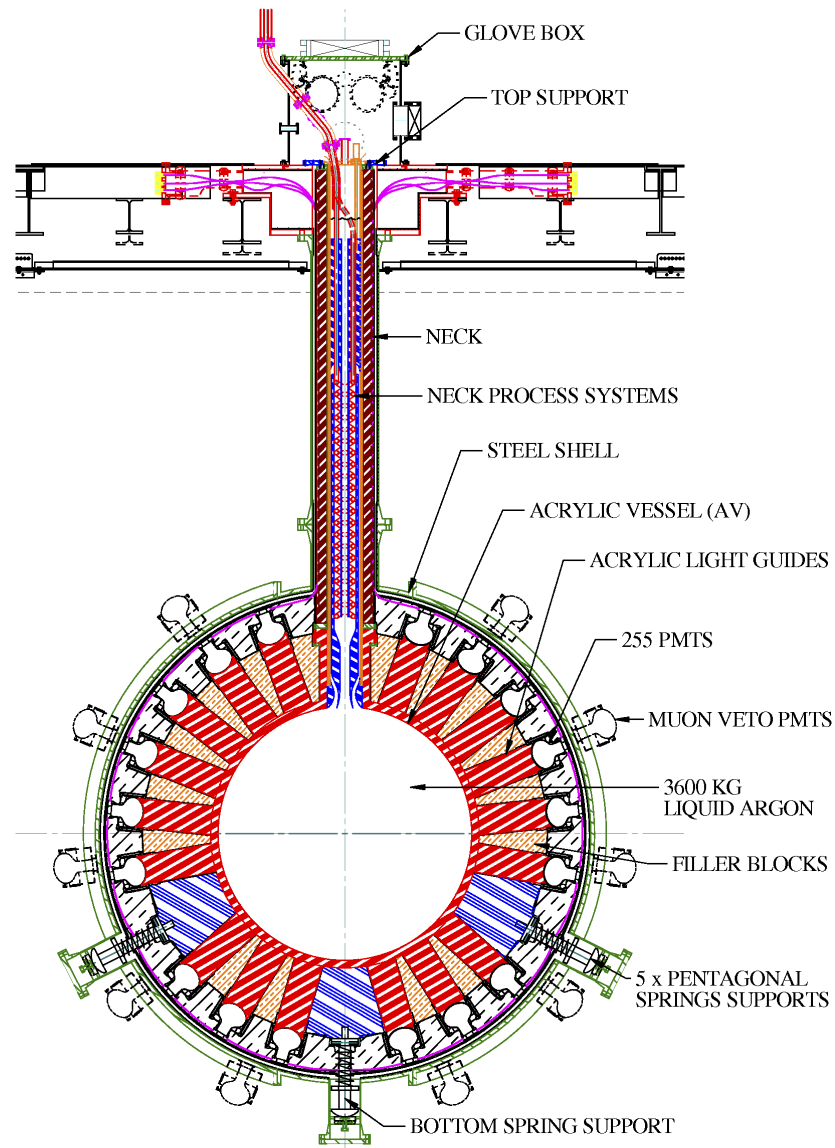


Figure 2.1: DEAP-3600 consists of 3600 kg of liquid argon in an acrylic vessel (AV). Scintillation light is shifted to the visible range with TPB on the inside of the AV. The light travels through 255 acrylic light guides to PMTs. The light guides provide shielding from neutrons from the PMTs, and also thermal insulation. Filler blocks made of high density polyethylene and polystyrene occupy the space between the light guides. The steel shell acts as a containment vessel. On the outside of the steel shell are 48 muon veto PMTs to detect Čerenkov radiation in the surrounding 8 m diameter water shield tank.

Chapter 3

Backgrounds

In a rare event experiment, such as a direct dark matter search, background control is of utmost importance. Unwanted background events in the detector can be confused with the WIMP signal, therefore all sources of background must be understood and controlled. DEAP-3600 requires the 20–40 keV_{ee} WIMP energy region of interest to be background-free. The acrylic vessel (AV) that contains the liquid argon target has stringent limits of 0.3 ppt ²³⁸U, 1.3 ppt ²³²Th, and 1.1×10^{-8} ppt ²¹⁰Pb. The radiopurity of the acrylic must be measured.

3.1 Classes of backgrounds

Backgrounds in DEAP can be organized into three groups: electromagnetic backgrounds, neutron backgrounds, and surface backgrounds. To achieve <1 background event in the fiducial volume in 3 years of livetime, a limit of 0.2 events is set for each of electromagnetic backgrounds, neutron backgrounds, and surface backgrounds. From each source of background, the limit is 0.01 events.

Electromagnetic backgrounds refer to beta and gamma events. The dominant source is the β^- decay of ^{39}Ar , a cosmogenically produced isotope. Argon from the atmosphere has an activity of approximately 1 Bq/kg [36]. Although these events are removed by PSD, using argon with less ^{39}Ar would reduce the background and allow a lower energy threshold. DEAP collaborates with groups from Princeton University and Fermilab, of the DarkSide experiment, who have extracted argon from underground that is depleted by a factor of >200 [37]. The first run with DEAP-3600 will use atmospheric argon, and a second run with depleted argon is anticipated.

It is expected that a WIMP will produce a signal that is indistinguishable from a neutron event; therefore neutron backgrounds must be reduced to extremely low levels. A study of every conceivable source of neutrons in DEAP-3600 investigated (α, n) reactions, spontaneous fission, neutron emission, (γ, n) reactions, and muon-induced neutrons [38]. The dominant source is (α, n) reactions, where an alpha interacts with a low mass element and a neutron is released. Alphas come from uranium and thorium impurities in detector materials, dust, or the rock walls, or from exposure to ^{222}Rn in the air. Radiopurity of materials is strictly controlled and measured. Impurities in the PMTs contribute the largest source of neutrons. To moderate neutrons that can not be eliminated, there is shielding of water and plastic.

Surface backgrounds refer to alpha decays from the inner surface of the detector. For a comprehensive report, see [39] and [40]. Both the alpha particle and the recoiling daughter nucleus can cause scintillation, in liquid argon and also in TPB [41]. The ^{238}U decay chain and ^{232}Th decay chain are long-lived and have many radioactive daughters. See Figures 3.1 and 3.2 [42]. The ^{238}U chain is particularly challenging, with ^{222}Rn and its progeny. Any ^{222}Rn decays quickly to ^{210}Pb with the emission of

3 alphas. The ^{210}Pb undergoes β^- decay to ^{210}Po , which is yet another alpha emitter. The half-life of ^{210}Pb , 22.20 years, causes a background that persists throughout the lifetime of an experiment.

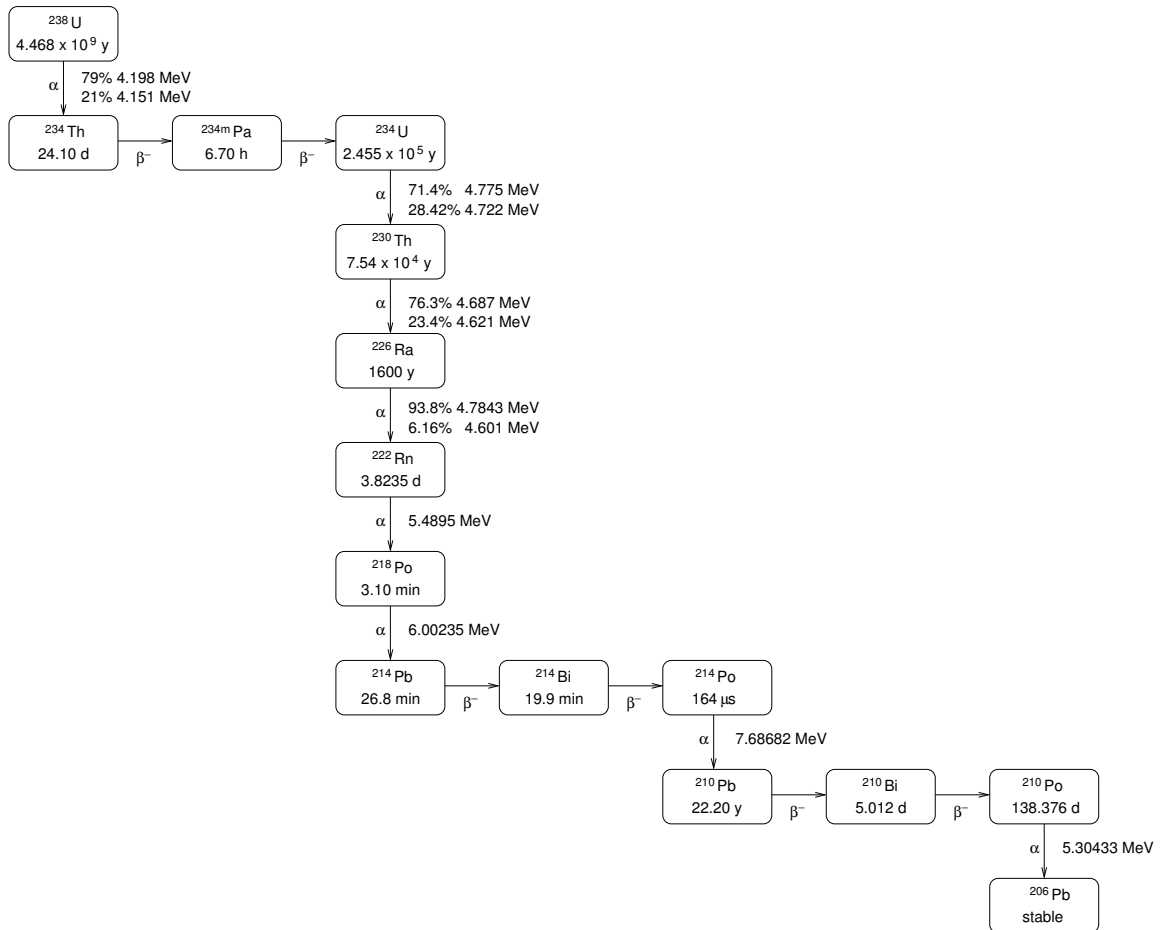


Figure 3.1: There are 8 alphas in the ^{238}U decay chain.

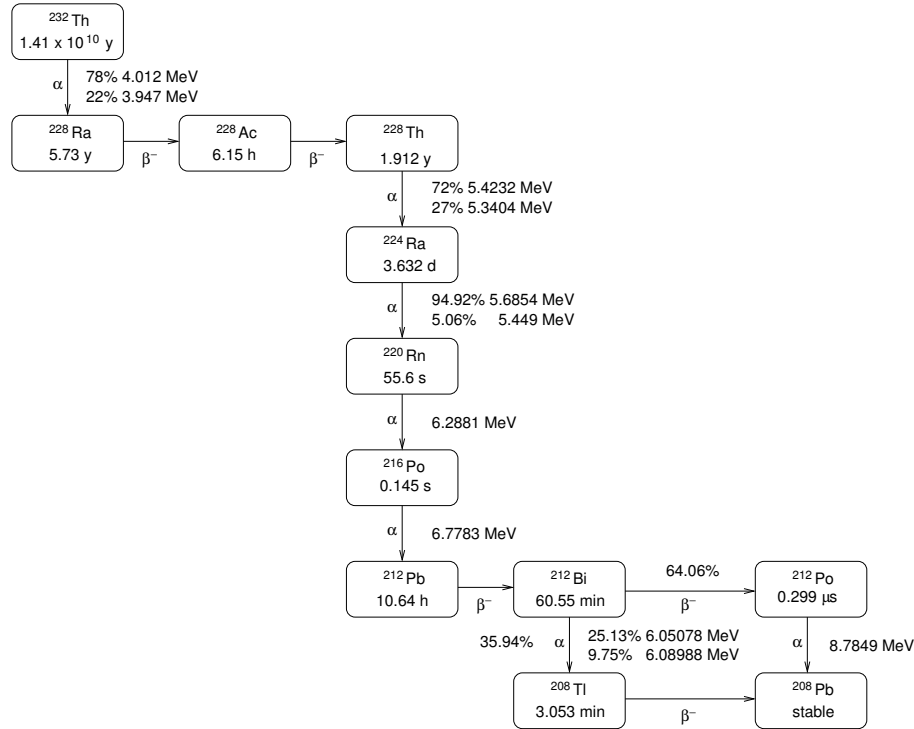


Figure 3.2: There are 6 alphas in the ^{232}Th decay chain.

An alpha decay that takes place entirely in the liquid argon can be identified by its high energy; however, if some of the energy is absorbed by the wall and only a fraction of the alpha energy is observed, or if the recoiling daughter nucleus is observed, the event will not be separated from a WIMP event. A recoiling daughter nucleus, with 100 keV, has a range of $<0.1 \mu\text{m}$ in acrylic or TPB [40]. The most energetic alpha, ^{212}Po from the ^{232}Th decay chain, with an energy of 8.78 MeV has a range of approximately $80 \mu\text{m}$ [43]. Fiducialization, considering the conservative estimate of 10 cm resolution on position reconstruction, reduces surface backgrounds by a factor of 1000 [40]. For even further reduction, surface roughness [44] and alpha PSD can be considered.

The main sources of surface backgrounds are: the TPB inner surface from the detector components, the AV inner surface from air exposure, the bulk TPB, and the bulk acrylic. Radon daughters plate out onto surfaces. Radon emanation from detector components, and contamination from the liquid argon, could contaminate the TPB inner surface. The AV, unlike the TPB surface, is exposed to ^{222}Rn in the air during detector assembly. Radon diffusion in acrylic is on the order of $100\ \mu\text{m}$ [45], and the ^{210}Pb daughter can be deposited to a depth of about 1 mm [46]. To remove the embedded ^{210}Pb , the inner surface of the AV will be sanded with a tool called the resurfacer. The resurfacer is lowered through the neck, and the arm can reach the entire inner surface. The surface will be sprayed with water, and the residue will be removed. The resurfacer is designed to remove 1 mm, which can be done twice if necessary [39]. During and after resurfacing, no air is permitted inside of the AV. The TPB and the acrylic used to make the AV must be exceptionally clean.

3.2 Requirements for the Acrylic Vessel

Manufacturing of the AV was carefully controlled for contamination [47]. The materials used to make acrylic have trace levels of ^{238}U and ^{232}Th . The greater concern is ^{222}Rn diffusion from air into the materials used to make acrylic. The acrylic manufacturing technique of slush casting, which involves a mixture of liquid methyl methacrylate (MMA) and beads of poly(methyl methacrylate) (PMMA), was avoided since the high surface area of PMMA beads leads to more ^{222}Rn diffusion and subsequent ^{210}Pb contamination. In addition, the beads may have been exposed to air for a long period of time. Liquid MMA has less exposure to air, and is used soon after production. The acrylic must be made from pure MMA monomer. The amount of air

used during distillation of MMA is used to estimate ^{222}Rn exposure. Thai MMA Co., Ltd. supplied the methyl methacrylate (MMA) monomer to RPT Asia, Ltd., which is also in Thailand. While in a storage tank the MMA was stirred, therefore any contamination would be distributed evenly throughout the volume. In a cleanroom, the liquid was poured into moulds to form 128 inch \times 96 inch \times 4.5 inch flat panels. Besides pure MMA, the acrylic contains 2% proprietary additives. The panels were sent to Reynolds Polymer Technology (RPT), Inc. in Grand Junction, Colorado. Five panels were thermoformed into gores and then bonded together. Next, a bottom piece was bonded on. The University of Alberta received the parts of the AV and machined out approximately 2 inch stubs where the light guides attach. The AV was shipped underground to SNOLAB as three components: the truncated sphere, the collar, and the neck. The dimensions of the truncated sphere were limited by the vertical shaft and the horizontal drifts in the mine. A custom shipping container was slung under the cage. The AV was annealed, which relieves any stress. For this purpose, a large oven was constructed underground. An anneal consists of slowly warming the AV, maintaining 90°C for 12 h, and then slowly cooling. Because radon diffusion increases as temperature increases, air low in ^{222}Rn was used to purge the AV during annealing and the ^{222}Rn concentration was monitored. After annealing, RPT travelled underground to SNOLAB to bond the collar to the truncated sphere. Bonding syrup is liquid MMA, PMMA beads, and some proprietary initiators. There was then a second anneal. The neck was bonded to the collar by RPT and then there was a third anneal. Finally, the 255 light guides were bonded to the AV. There was another anneal. Estimating the contamination at each stage of AV construction would not have been possible without cooperation from the manufacturers.

The background requirement is <0.01 events from the inner $80\ \mu\text{m}$ of the bulk acrylic. Table 3.1 shows the maximum tolerable concentrations for ^{238}U , ^{232}Th , and ^{210}Pb , as calculated by a Monte Carlo model [40]. Secular equilibrium is assumed for the ^{238}U and ^{232}Th limits. The ^{210}Pb limit is 8.4 times the equilibrium ^{238}U level.

Table 3.1: Limits in bulk acrylic

	($\mu\text{Bq/kg}$)	(g/g)
^{238}U	3.7	0.3×10^{-12}
^{232}Th	5.3	1.3×10^{-12}
^{210}Pb	31	1.1×10^{-20}

3.3 Assay techniques

Although ^{210}Pb in acrylic has never before been measured, SNO measured ppt levels of ^{238}U and ^{232}Th in acrylic. The following summary is from the SNO Technical Reports. Each sheet of acrylic used in the SNO AV was measured and found to be at least an order of magnitude lower than the targets of 7 ppt ^{238}U and 2 ppt ^{232}Th . Various techniques were explored including neutron activation and gamma spectrometry; alpha spectrometry; and mass spectrometry as thermal ionization mass spectrometry (TIMS) or inductively coupled plasma mass spectrometry (ICP-MS). Acrylic vaporization was required to concentrate the activity.

The preferred technique, with the least amount of contamination due to handling, consisted of neutron activation, vaporization, and gamma spectrometry by a well detector at Chalk River Laboratories (CRL). Lawrence Berkeley Laboratory and Queen's University assisted with gamma spectrometry as well. Los Alamos National Laboratory investigated neutron activation and a vaporization technique with a well

detector and anti-Compton shield. At the same time, vaporization followed by TIMS was tested by the National Bureau of Standards (NBS) in Gaithersburg, Maryland. A complete acrylic vaporization system was designed by CRL. The acrylic block was placed in a cylindrical boat made of Suprasil, an ultrapure synthetic quartz, and vaporized at 500°C in a N₂ atmosphere. A large sample, up to 25 kg from sequential vaporization of 1 kg blocks, was concentrated into a residue which was then removed from the Suprasil boat by rinsing with ultrapure acids. Combinations of aqua regia, hydrochloric acid, nitric acid, perchloric acid, and hydrofluoric acid were investigated. Infrared lamps were used to achieve 85–100°C during each of the two 1 h rinses. The National Research Council (NRC) research facility in Ottawa, ON performed ICP-MS. At CRL, the effluent was analyzed by TIMS and by alpha spectrometry. For alpha counting using a silicon detector, the U, Th, and Ra were separated and electroplating was used to deposit each element on a stainless steel disc. From this technique, it was concluded that there was no disequilibrium in the ²³⁸U and ²³²Th decay chains. Neutron activation, alpha spectrometry, and mass spectrometry all reached a sensitivity at the 0.5 ppt level. It was found that the mass spectrometry and alpha spectrometry results agreed, yet were significantly higher than the neutron activation results. Even with some handling contamination, all results were below the targets. Complete with blanks, tracers, and spikes, acrylic from several manufacturers was evaluated. SNO developed an extensive program for the radiopurity measurement of acrylic to confirm the reliability and agreement of different techniques.

Other materials have been assayed for ²¹⁰Pb, including low concentrations in environmental samples such as water, soil, and animal tissue. Unlike for ²³⁸U and ²³²Th, neutron activation is not an option for ²¹⁰Pb due to a very low cross section [48].

A measurement of ^{210}Pb may involve radiometric or mass spectrometric methods. Concentration, and also separation of Pb, may be necessary. Detection limit, time, and effort are important factors. The common radiometric techniques for ^{210}Pb are to measure the 46.5 keV gamma from ^{210}Pb , the 1.2 MeV beta from ^{210}Bi , and the 5.3 MeV alpha from ^{210}Po . In a study of ^{210}Pb in environmental samples, after heating in 550°C air for 6–8 h, all three techniques were found to agree [49]. Alpha spectrometry had the lowest detection limit, followed by beta counting, then gamma spectrometry. In contrast, gamma spectrometry was the fastest, then beta counting, then alpha spectrometry. In terms of sample preparation, gamma spectrometry required the least effort, then alpha spectrometry, then beta counting. Perhaps the detection limit for gamma spectrometry would have been improved with the use of a well type high purity germanium (HPGe) detector. Inductively coupled plasma mass spectrometry (ICP-MS) with concentration and separation reduces the time requirement, and has been shown to agree with gamma spectrometry [50]. The choice of technique depends on the specific measurement to be undertaken.

SNOLAB has a well-established gamma assay program with a 200 cm^3 coaxial detector from PGT, Princeton Gamma-Tech Instruments, Inc. This detector has a sensitivity of approximately 10 ppt for ^{238}U and ^{232}Th [40]. However, a coaxial detector cannot detect the low energy gamma from ^{210}Pb . An offcut from the AV was measured to have <8.4 ppt ^{238}U and (41 ± 42) ppt ^{232}Th [51]. In any event, a more sensitive assay was required for the ^{210}Pb measurement.

The DEAP acrylic assay is based on the vaporization technique used by SNO. To measure the radiopurity of acrylic at such extremely low levels, a large quantity of acrylic was vaporized and the concentrated lead-containing residue was collected by

rinsing with heated acids. The ^{210}Pb was measured with a well detector, and also by its ^{210}Po daughter with an alpha counter. Count rates can be increased by vaporizing more acrylic.

The acrylic assay can be compared to a study of ^{210}Pb and ^{210}Po from caribou muscle and reindeer bone, in which 1–2 g samples were heated in a furnace for 24 h [52]. The residue was dissolved in heated concentrated nitric acid and 73% perchloric acid. There was no loss during rinsing. The ^{210}Po was collected on a disc and measured with a ZnS(Ag) scintillation counter. To measure the ^{210}Po from the sample, the sample was counted right away. To measure ^{210}Pb from the sample, the sample was stored for 4–6 months to allow ^{210}Pb to decay to ^{210}Po . Then the ^{210}Po was collected and counted. The samples were measured to be on the order of 10^{-15} g/g ^{210}Pb . Several temperatures were investigated and compared to the result from 100°C . In muscle, the recovery of ^{210}Po decreased quickly from 97% at 150°C , to 60% at 200°C , to 7% at 300°C . In contrast, bone showed 90% up to 250°C , and 70% at 500°C . Therefore, it is evident that the matrix affects volatilization. For ^{210}Pb recovery, the first statistically significant result in muscle was $(40 \pm 22)\%$ at 300°C ; however, there may have been loss at as low as 150°C . In bone, the ^{210}Pb recovery was 95% at 500°C , 79% at 700°C , and 3% at 1000°C . In general, a temperature of 500°C is recommended for good ^{210}Pb recovery [48]. Elsewhere, detection limits of 7×10^{-17} g ^{210}Pb [53] and 10^{-19} g/g ^{210}Pb [54] have been reported.

Another technique being developed by DEAP is ^{210}Pb detection based on beta-gamma coincidence [55]. Within 3 ns of the 63.5 keV beta from ^{210}Pb , the 46.539 keV gamma is emitted [42]. Following vaporization and rinsing, the effluent is evaporated to dryness and collected in 0.1 M HNO_3 . The sample is shipped from SNOLAB to

Royal Holloway, University of London (RHUL) where it is mixed with liquid scintillator. At Boulby Underground Laboratory, the sample is placed between two acrylic light guides with PMTs and two planar HPGe detectors. Currently, the system is being calibrated with a ^{210}Pb source.

Chapter 4

The acrylic vaporization system

Located on surface at SNOLAB, the acrylic vaporization system is the core of the acrylic assay. The thermal degradation of acrylic, poly(methyl methacrylate) (PMMA), produces methyl methacrylate (MMA) vapour. The MMA vapour has a very unpleasant odour, therefore the acrylic vaporization system is designed for pyrolysis of acrylic followed by removal of MMA by combustion. The system consists of two large furnaces, for vaporization and incineration. A piece of acrylic is placed in a cylindrical boat, inside the vaporization furnace. While acrylic vaporizes, lead remains in the boat. Air is injected into the incineration furnace and the MMA burns. To remove char in the boat, air is added to the vaporization furnace after vaporization is complete. The acrylic vaporization system can accommodate 2 kg each day; however, on the order of 10 kg is required to increase count rates. There is an option to sequentially vaporize five 2 kg blocks in the same boat. After vaporization, the boat is rinsed with heated acids to collect the concentrated residue for counting. A well detector is sensitive to the 46.5 keV gamma from ^{210}Pb . An alpha counter is used to measure the 5.304 MeV alpha from the ^{210}Po daughter.

4.1 Vaporization

4.1.1 Procedure

A block of acrylic, 6 cm \times 6 cm \times 50 cm with a mass of 2 kg, is cut on a dedicated King Industrial cabinet saw. Cleaning the acrylic sample involves wet sanding, first with water and then with an Alconox solution, 10.0 g in 1 L ultrapure water (UPW). The sanding is done by hand with sandpaper. The block is sprayed with UPW before being soaked in a Radiacwash solution, 1:40 Radiacwash and UPW, for 20 min. Finally there are two rinses with UPW, each 20 min long. The plastic basin requires approximately 10 L to submerge a 2 kg block. Because the bottom face of the acrylic rests on the container and is not necessarily in contact with the solution, the block is rotated after 10 min of each 20 min rinse. The block quickly dries, although Kimwipes or N₂ gas may be used. The block is weighed on an electronic balance and is then sealed in a plastic bag.

The acrylic vaporization system is at SNOLAB, on surface. There are doors to separate the area used for acrylic vaporization from the machine shop. The system consists of two Thermo Scientific Lindberg Blue HTF 55000 series hinged tube furnaces, each 1.2 m in length, one each for vaporization and incineration. See Figure 4.1 for a photo and Figure 4.2 for a schematic. The acrylic is placed in a 75 cm cylindrical boat made of Suprasil, an ultrapure synthetic quartz. To contain the acrylic when it melts, the ends of the boat have been flared inward by a glassblower. The opening at one end is large enough to load the acrylic block, 8.5 cm in diameter, while the downstream end is smaller to prevent liquid from overflowing, 4 cm in diameter. The boat sits inside of a quartz tube in the vaporization furnace. The quartz tube is 15 cm

in diameter and 1.5 m in length with a wall thickness of 4.5 mm. While being flushed with a continuous flow of N_2 gas the vaporization furnace is heated to 400°C , then 500°C . The N_2 gas is boilloff from a large liquid nitrogen storage tank, because it is a convenient supply but also in the interest of radiopurity. It is important to emphasize that radiopurity was always under consideration during design and installation of the acrylic vaporization system. High purity valves and tubing, often Swagelok, were selected.



Figure 4.1: The acrylic vaporization system is on surface at SNOLAB. Acrylic is vaporized in the furnace on the left, and the MMA vapour is incinerated in the furnace on the right [56].

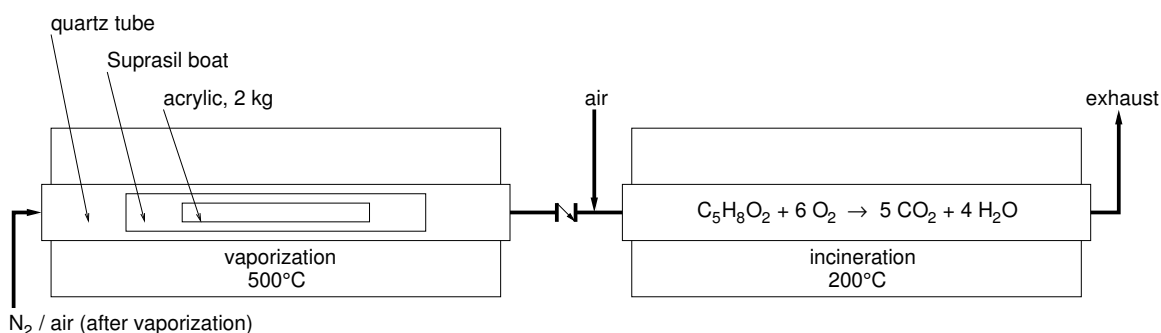


Figure 4.2: The acrylic vaporization system first vaporizes PMMA in an N_2 atmosphere, and then destroys MMA by incineration. A block of acrylic is contained in a cylindrical Suprasil boat. Air is added to the incineration furnace. After vaporization is complete, carbon is removed from the boat by injecting air into the vaporization furnace.

It is generally accepted that when heated the PMMA polymer tends to break up into its MMA monomer. The boiling point of MMA is $(100.6 \pm 0.2)^\circ\text{C}$ [57], therefore the primary product of vaporizing acrylic is MMA vapour. The odour is very unpleasant, but exposure to MMA is not considered a hazard. Humans can smell MMA at 0.05 ppm [58]; however, the Ontario Ministry of Labour states 50 ppm for the time-weighted average limit (TWA), which can be considered the allowed concentration [59]. In the event of a leak of MMA vapour indoors, a Matheson-Kitagawa Toxic Gas Detector System was available to measure MMA at 10–160 ppm. Recall that this acrylic vaporization system was designed to eliminate the annoying odour. It was deemed acceptable during the SNO experiment to release the MMA vapour outdoors.

The lids of the furnaces may be opened to observe the vaporization or incineration. In fact, a counterweight was installed in order for a lid to be easily opened and kept open, therefore minimizing the risk of burns. Figure 4.3 shows the acrylic block in

the boat before vaporization has begun. Around 300°C, the sounds of tiny bubbles popping can be heard. The surfaces of the block begin to melt, made visible by the softening of the edges. The bubbles become larger on the surface. Liquid drips or splatters, and bubbles are seen in liquid that has pooled. See Figure 4.4. In some samples, the acrylic is foamy. Again, depending on the manufacturing, the solid and liquid acrylic changes from colourless to yellow. The vapour is white in colour. Provided the vaporization is progressing as expected at 400°C, the temperature is increased to 500°C. Vaporization of a 2 kg block takes approximately 3 h, which is followed by an hour-long N₂ purge.



Figure 4.3: A 2 kg acrylic block is placed in the boat, and the boat is loaded before the vaporization furnace is turned on.



Figure 4.4: The DEAP-3600 AV acrylic from RPT turns yellow, drips, splatters, and produces black char. The block slides downstream due to an intentional incline. (a) 20 min and (b) 30 min after the start of vaporization.

Through what is called the transfer section, the MMA vapour flows from the vaporization furnace to the incineration furnace. There is a 0.5 psi check valve surrounded by two 10 psi pressure relief valves which vent to outside. Sanitary Tri-Clamp fittings are used for connections. To prevent blockages, all components of the transfer section have a large diameter. For example, the pressure relief valves are $\frac{3}{4}$ inch and the attached hoses are 1 inch. Three separate holes were punched into the machine shop wall for the pressure relief valve lines and the exhaust line. The transfer section must be maintained above 100°C to prevent MMA from condensing. Wrapped around the check valve are heated sleeves that are set to 60 V through a Variac. Six resistance temperature detectors (RTDs) are placed at various locations of the transfer section: typically at the outlet of the vaporization furnace, on each of the pressure relief valves, on the check valve, in between the check valve and the incineration furnace, and at the inlet to the incineration furnace. The furnaces and the transfer section were installed on an incline so any liquid MMA that condenses flows into the incineration furnace.

After the check valve, air from an air compressor in the warehouse is injected into the incineration furnace to provide oxygen for combustion. Complete combustion of MMA follows $C_5H_8O_2 + 6 O_2 \rightarrow 5 CO_2 + 4 H_2O$ [60]. The incineration furnace is filled with steel wool to provide a large surface area and is operated at 200°C. The vapour, thick and white, is observed at the inlet but not inside the incineration furnace. The products move to the exhaust line. A fan is directed at a large coil of copper to allow water vapour to condense. The dripping of liquid into the steel drum can be heard. The remaining gases are vented through a 1 inch diameter galvanized steel pipe. It can be confirmed that there is no white vapour leaving the vents by looking outside.

An excessive amount of char accumulates in the boat. Consider the structure of

MMA, $\text{CH}_2=\text{C}(\text{CH}_3)\text{COOCH}_3$ [61]. The char is produced by the scission of the C–C bond of the carbonyl side group [62]. The CO_2 and CH_4 are volatile, and the char remains. It has been estimated that much as 15% of the initial mass of PMMA is left as char [62]. In an early commissioning run, we filtered, dried, and measured the char from an (84.8 ± 0.1) g sample of scrap acrylic to be (0.4 ± 0.1) g, or $(0.5 \pm 0.1)\%$ of the initial mass. A 10 kg run would correspond to at least 50 g, and maybe even 1500 g of char. This solid material would make rinsing and counting difficult. To remove carbon, after vaporization is complete, air is added to the vaporization furnace for 1 h. Carbon combines with oxygen to form carbon dioxide that goes to the exhaust, $\text{C} + \text{O}_2 \rightarrow \text{CO}_2$. See Figure 4.5. A small amount of carbon, as black particles, remains on the boat. At the end of the run, the furnace lids are opened and the system is cooled off with N_2 flowing at the maximum flow rate for 1 h. The system is left to cool overnight.



Figure 4.5: Acrylic vaporization produces too much char to manage during rinsing and counting. (a) The entire boat is covered and becomes opaque from 2 kg of the RPT acrylic used for the DEAP-3600 AV. (b) After vaporization, air is added to the vaporization furnace to remove the char.

4.1.2 Commissioning

The acrylic vaporization system has been used for 35 vaporizations. Starting with approximately 10 g pieces, the mass of the sample was gradually increased to full-scale 2 kg blocks. These commissioning runs used scrap acrylic, sometimes from SNO or from McMaster-Carr. It was observed that some samples of acrylic behave differently. Often the source of the acrylic was unknown, and the behaviour could be difficult to understand while we tried to tune parameters of the acrylic vaporization system, for example, the temperature or the flow rate. The vaporization of the RPT acrylic was quite unexpected. Unlike other samples, the RPT acrylic foams and expands during the initial stages of vaporization. The liquid is very yellow in colour, instead of white and transparent. There is more splattering on the sides and top of the boat, and also much more char. The literature on the thermal degradation of PMMA also exhibits discrepancies, which can be attributed to the conditions during polymerization [63, 64].

To observe the products of vaporization in the transfer section, a Pfeiffer OmniStar GSD 301 O3 gas analysis system was used qualitatively. The purpose was to determine when to add air to the vaporization furnace, by waiting until no more MMA was detected. It was also interesting to observe the peaks from N₂ at 28 amu, O₂ at 32 amu, Ar at 40 amu, and MMA at 100 amu. It is not uncommon to see other products in addition to the monomer, and it is possible for MMA itself to degrade [64, 65]. A peak at 69 amu, due to CH₂C(CH₃)CO [64], was particularly easy to notice in the spectrum. Unfortunately, the OmniStar required repair and is no longer used with the acrylic vaporization system.

The operating pressure was initially a challenge. The furnaces, with their quartz

tubes sealed with flanges, were not designed for positive pressure. The flanges, consisting of silicone O-rings around the quartz tube, would slowly be pushed off the end of the tube. A steel plate was added to hold the flange, but because it was only at the bottom of the flange, there was still a problem at the top. The solution was to install two stainless steel threaded rods, along the entire length of the quartz tube, to hold the flanges at each end together. A low operating pressure of 5 psi was selected to begin with; however, spikes in pressure were observed as MMA was incinerated. The pressure relief valves were therefore adjusted from 5 psi to 10 psi. In the early stages of commissioning, there were often leaks of MMA, both vapour and liquid, yet at such low concentrations that they could not be measured by the Matheson-Kitagawa detector tubes. Two PTFE bellows were responsible for the leaks and were removed. Even with additional hose clamps around the PTFE bellows, the leaks persisted. At the vaporization furnace, liquid in the boat flows towards the transfer section. In some larger mass samples, 800 g for example, the liquid MMA overflowed out of the boat and into the quartz tube. The Suprasil boat had to be modified to have a smaller opening at that end.

Heating the transfer section to 100°C continues to be an issue. Although heating tapes were effective at reaching the temperature, they would crack and burn no matter the configuration. Instead, two heated sleeves are wrapped around the top and bottom of the check valve. Because the sleeves do not fit tightly around the transfer section, the ends are plugged with a pair of heat resistant gloves. Typically it takes 3 h to preheat the transfer section; however, if the sleeves and gloves are not assembled perfectly it becomes very difficult to reach 100°C. The way in which the transfer section is heated should be improved. The RTDs are effective at measuring

the temperature throughout the transfer section. They cannot be placed on the quartz tubes or on the flanges since the adhesive burns and the RTD must then be replaced. The maximum temperature of the temperature monitor is 256°C. Another modification was required after fire was noticed where air was added at the transfer section. As a result, the silicone gaskets became damaged and liquid would leak out. While replacing the gaskets, we noticed accumulation of both liquid and solid products that were a concern in terms of a blockage in the transfer section. A change was made to inject air through the inlet flange of the incineration furnace.

The incineration process is not fully understood. Originally the incineration furnace was operated at 800°C, in order to be above the 421°C autoignition temperature of MMA [58]. Sometimes as the furnace heats up, a loud bang is heard. It is presumably from the expansion of materials in the furnace and is not a problem, but can be alarming. The silicone O-rings on the incineration furnace have melted but still seal; they could be replaced. There is an option to insert alumina foam blocks in the incineration furnace to prevent the O-rings from becoming too hot.

During the first vaporizations, of 10–100 g, there were no indications of issues at the incineration furnace. It was quite impressive to observe flashes of flames in the incineration furnace. With the later samples, for example with 1500 g, there was concern that complete combustion was not being achieved. Smoke could be seen outside and one of the products, a liquid that has not been identified, accumulated in the exhaust line. The flowmeter would fill up with the liquid, and had to be removed. That line was capped and the valve was closed to be able to use the alternate path through the 0.3 psi check valve. There is a distinct odour at the water trap and in the exhaust line, and it seems to be different than MMA. It was thought that the odour

was leaking from the water trap, a plastic container connected with Tygon tubing. Our initial attempt to use the refrigerated Titan Vacuum Vapor Trap to collect water was unsuccessful. Unfortunately, the Titan Trap is not designed for positive pressure either, and vacuum grease and bungee cords did not solve the problem of the lid popping off. The water trap was finally improved by replacing the Tygon with a coil of copper tubing and the plastic container with a steel drum. One suggested explanation for the liquid and smoke was that there were some chemicals used during manufacturing of the steel wool that is in the incineration furnace. Perhaps the high temperature was responsible for the degradation of MMA to other hydrocarbons. To test this, a run was done with the incineration furnace set to 200°C. No smoke was observed outside. The MMA vapour could be seen entering the incineration furnace, and then it was eliminated. We have continued to run the incineration furnace at this lower temperature for the last six vaporizations. The flow rates should be optimized next. Currently the flow rates are set, almost arbitrarily, to 45 units or 2.6 L/min at the N₂ flowmeter (150 units = 8.505 L/min), and 60 units or 18 L/min at the air flowmeter (150 units = 45 L/min). To summarize, the incineration process requires further investigation. Regardless, incineration is secondary to the physics goals related to vaporization.

After two years and 35 vaporizations, the acrylic vaporization system should be cleaned. The quartz tubes are longer than the furnaces, and where the ends extend away from the heat becomes coated in products from the vaporization. Normally the inlet of the vaporization furnace quartz tube is wiped with Kimwipes and methanol. The other end of the vaporization furnace quartz tube and the quartz tube in the incineration furnace are rarely cleaned. A stronger solvent, like acetone, or even

hydrochloric acid could be used. There has also been a suggestion to enclose the acrylic vaporization system in a cleanroom, within the SNOLAB machine shop.

4.1.3 Safety

Safety was the top priority during the design and commissioning of the acrylic vaporization system. Significant modifications required approval¹ and for the flowsheet to be updated [66]. A reviewer signs off on the operating procedure as well [67]. A safety review committee² was involved during the early stages of commissioning. First, the hazards were evaluated and mitigation strategies were planned. The hazards associated with operation of the acrylic vaporization system are explosion, fire, burns, and MMA exposure. See the hazard assessment for more detail [68]. The flashpoint of MMA is 10°C, and the explosive limits are 1.7% and 8.2% [58]. Explosion conditions could be established after a pressure buildup that damages components and allows MMA to mix with air. A blockage could result in overpressure, and so could the production of too much vapour. For a 2 kg block of acrylic, 440 L of vapour are produced [65]. In addition to the pressure relief valves in the transfer section, 10 psi check valves serve as pressure relief in the N₂ and air lines. The procedure includes a test to confirm that the pressure cannot be increased beyond 10 psi. There is also an 8 psi pressure test to identify leaks over 10 min. A fire could start because of a leak that allows MMA to come into contact with air, or because of a furnace overheating. The furnaces have Auber SYL PID temperature controllers that are used to choose the set value and the high alarm, in addition to many other parameters. If the furnace

¹I would like to thank Oleg Li for tolerating the many changes to the engineering drawing.

²Thanks to the acrylic vaporization system review committee, which involved Allan Barr, Richard Ford, Tom O'Malley, Nigel Smith, and James Waite.

failed, exceeded the set value, and reached the high alarm, the heating element of the particular zone that failed would be turned off. It was preferable to have the entire furnace shut down in such a situation, and so each furnace was rewired. An emergency button that turns off both furnaces was also incorporated. The machine shop is equipped with a fire detection and alarm system. In the event of a fire, evacuation is most important. Only if there is an evacuation path and if the operator feels safe may they use the emergency button to shut off the furnaces or attempt to put out a small fire. There are Class ABC fire extinguishers at both exits. Obviously burns are a hazard since the furnaces and quartz tubes, transfer section, and exhaust line become very hot. Heat resistant gloves are available, and a lab coat can be worn to cover forearms. Finally, exposure to MMA is considered. Operators would only be exposed to MMA if there was a leak. MMA would be released to outside if the conditions for incineration were not met. In case there is a loss of N_2 or air flow, pressure alarms have been installed but are not yet in use. As a secondary supply, there are gas cylinders of N_2 and air. The vents were put at a height of 15 feet, high above human occupancy, and any MMA released would be quickly diluted. We expected, and now have demonstrated, safe operation of the acrylic vaporization system.

4.2 Acid rinse

The day after a vaporization, the boat is moved into the chemistry laboratory in the SNOLAB surface cleanroom. Acids are used to extract the residue, which contains the lead, from the boat. Because SNO measured high recovery efficiency using thorium and radium tracers [69], we anticipated good recovery of lead. However, in the interest of safety we chose to avoid the use of hydrofluoric acid and first evaluate aqua regia,

(3:1 vol/vol concentrated hydrochloric acid and concentrated nitric acid). Under a fume hood, the boat is placed on heated rollers and rinsed. See Figure 4.6. The Commercial Pro Roller Grill, CPRG50, rotates the boat at 1 rpm. The details of the acid rinse are in the chemistry procedure [70]. First, the boat is placed on the rollers and heated for 30 min. Aqua regia is prepared by pouring 12 mL of nitric acid into 36 mL of hydrochloric acid. It is allowed to react for about 1 min before being added to the boat. The colour changes from colourless, to yellow, to red-orange. A 50 mL beaker fits inside the larger end of the boat and is used to pour the aqua regia. Upon making contact with the residue, the aqua regia fizzes. Any white ash from vaporization is dissolved with one pass. The black particles, however, do not dissolve and stick to the walls. Throughout the rinse, vapours can be seen leaving the ends of the boat. The volume reduces drastically from 48 mL, typically to about 5 mL. There are two 1 h rinses with 48 mL of aqua regia, followed by a 5 min rinse with 20 mL of ultrapure water (UPW). The effluent from each rinse is collected in the same container.

If the sample is to be counted in the well detector right away, the effluent is poured into a polytetrafluoroethylene (PTFE) beaker. The volume can be reduced by evaporation by placing the PTFE beaker directly on a hot plate at 100°C. In the meantime, the 3 mL PTFE bottle to be used during counting is soaked in 60 mL of aqua regia for 1 h. A pipette is used to transfer the effluent into the 3 mL PTFE bottle. The sample is then transported underground to be counted. The 3 mL PTFE bottle is kept in a 30 mL polypropylene Nalgene bottle in case of leaks and for a barrier against ^{222}Rn . That is sealed in a plastic bag, and then double bagged. If the sample is not going to be counted in the well detector right away, the approximately

20 mL can be stored in a fluorinated ethylene propylene (FEP) bottle.



Figure 4.6: The residue from vaporization is removed from the boat by rinsing with aqua regia. (a) The boat rotates and is heated. (b) Aqua regia is poured into the boat and reacts for 1 h before being collected. The aqua regia rinse is repeated, and finally there is a quick rinse with UPW.

Revisions were made to the procedure as we gained experience with rinsing. Aqua regia is very aggressive. We first learned that the Nalgene counting pots are not compatible with aqua regia; the colour changed to brownish yellow and all of the liquid eventually evaporated from within the closed container. Containers made of FEP and PTFE are unaffected [71]. Aqua regia has corroded the stainless steel body and rollers of the roller grill, especially at the small end of the boat where vapours are released, and the rust has to be cleaned up frequently. Perhaps the rollers should be replaced, but its likely that the new ones would be quickly damaged as well.

I would suggest using a larger volume of aqua regia, >48 mL, for the rinses. The volume reduces to such a small volume after an hour-long rinse, and likely depends on the residue from vaporization that reacts with the aqua regia. A few millilitres are

expected, but there have been samples that leave only a few drops or nothing at all. The volume of 50 mL was selected because it is a small volume that still covers the length of the boat. It was determined that the boat holds 700 mL. During this test, UPW did not spill out of the boat until the last 50 mL of 750 mL. That being said, it is difficult to pour a larger volume from the boat. It is best to hold the boat vertically so liquid cannot run back along the bottom of the boat. This is possible with small volumes, but even 20 mL can be hard to manage. I have spilled several times, and the loss can mean the entire vaporization needs to be repeated. The boat design could be modified to have a pouring spout. It has also been suggested that the effluent be pipetted from the boat, instead of poured. A more thorough final rinse of the boat by spraying UPW from a bottle should be included in the procedure. Sometimes not all of the particles that are on the walls of the boat are collected.

Some investigation of the ideal temperature of the aqua regia would be beneficial. After 1 h, a thermometer measured about 45°C. The temperature could be increased, if necessary, with heat lamps. The duration of the rinses could be explored. Measurement of the temperature while the volume is being reduced on the hot plate could also be improved. Currently, an RTD wire is placed on the hot plate and is read out by a multimeter. It can be difficult to make good contact with the hot plate, and the reading can fluctuate greatly. The hot plate setting always seems to be much higher than what is measured by the RTD. For example, the temperature must be increased to 190°C on the hot plate for the RTD to read 100°C. The effluent is now evaporated directly on the hot plate, yet to begin with, the effluent was first neutralized with sodium hydroxide. Such a large quantity was needed that the sodium chloride would often come out of solution as the volume was reduced. A water bath, made with

UPW, was considered for the volume reduction, but it was suggested that if UPW condensed in the sample container, any impurities in the UPW could contaminate the sample. Without measuring these radiopurity issues, it is difficult to suggest what measures are necessary. Often it is better to be careful and choose the cleanest option; however, financial aspects must also be considered. Ultrapure chemicals, both hydrochloric acid and nitric acid, were purchased. Labware that is cleaner than glass, for example, PTFE or polyethylene as was used by SNO [69], may be required.

Chapter 5

Gamma spectrometry

The effluent was measured in an ultralow background high purity germanium (HPGe) well detector underground. A well detector is specifically intended for low energy gamma spectrometry. The sample is placed inside of the germanium crystal and almost 4π counting is achieved. It has high efficiency and low background for the 46.5 keV gamma from ^{210}Pb . As an example, well detectors have been used to measure ^{210}Pb in water [72]. A custom well detector [73] was purchased for this measurement. The 300 cm³ well detector, EGPC 292-P21 No. 54206, is LN₂ cooled with the cryostat, SB 99-30A-T2FA No. 1332. The well has a diameter of 21 mm and a depth of 66.5 mm. The 3 mL PTFE bottle from Cowie Technology Corp. was selected because it fits in the well detector, with a height of 3.4 cm, a diameter of 2.0 cm at the base, and a diameter of 1.0 cm at the neck.

To shield from local radioactivity, the well detector is enclosed in shielding purchased from Canberra. Outwards from the centre, there is 5.0 cm of copper, 5.0 cm of lead that is low in ^{210}Pb , and 22.35 cm of regular lead. The centre core of copper consists of 10 rings that stack together. Before shipping underground, the copper rings

were removed, cleaned, and sealed in bags in order to prevent exposure to radon in the air. The activity of ^{222}Rn is $(131 \pm 7) \text{ Bq/m}^3$ underground [74], and $(7 \pm 2) \text{ Bq/m}^3$ on surface [75]. Inside of the shielding, the well detector is flushed with boiloff N_2 gas from a dewar of LN_2 at a rate of 2 L/min. Gas cylinders have been used instead, but they do not last as long as a LN_2 dewar. Both gas cylinders and boiloff N_2 from a LN_2 dewar have about 0.5 mBq/m^3 ^{222}Rn [76]. The shielding and nitrogen flush reduce the backgrounds in the well detector.

5.1 Performance

An example of the quality of the data from the well detector is shown in Figure 5.1. The resolution was as expected. A window for the ^{210}Pb peak was set as 44.5–48 keV. There were 600 counts in about 8 d, or $(77 \pm 3) \text{ cpd}$.

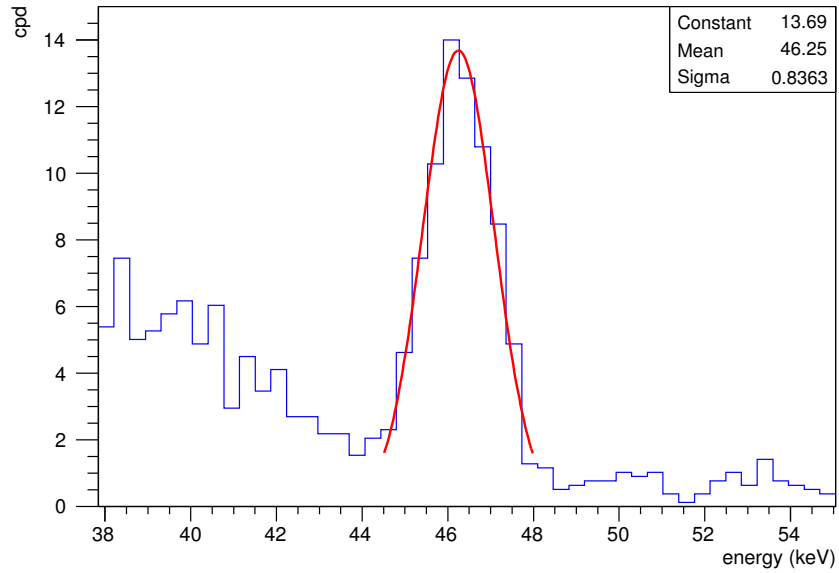
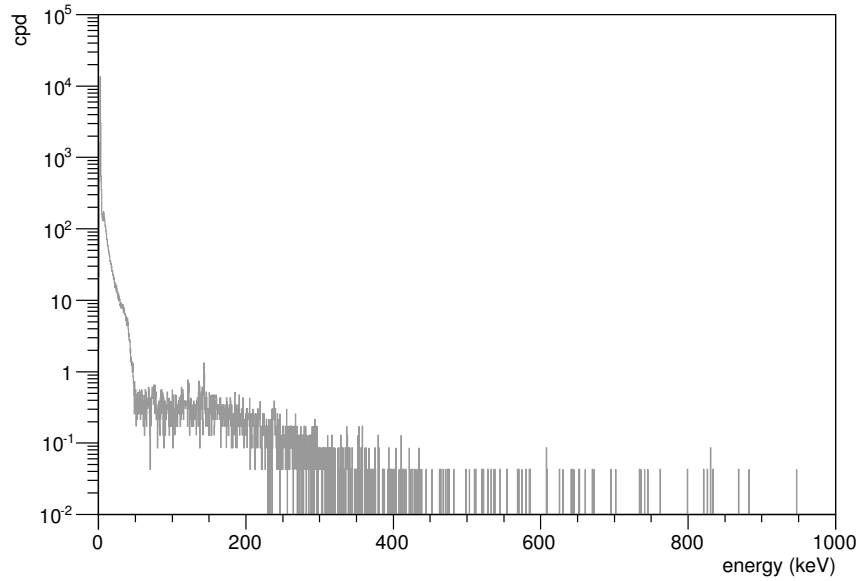


Figure 5.1: A Gaussian fit of the ^{210}Pb peak gives a FWHM of 2 keV. Note that this sample is not part of the acrylic assay.

5.2 Background

In a recent evaluation of the background, the empty well detector collected data for 23 d. See Figure 5.2. There is no clear peak at 46.5 keV.



(a) Full spectrum

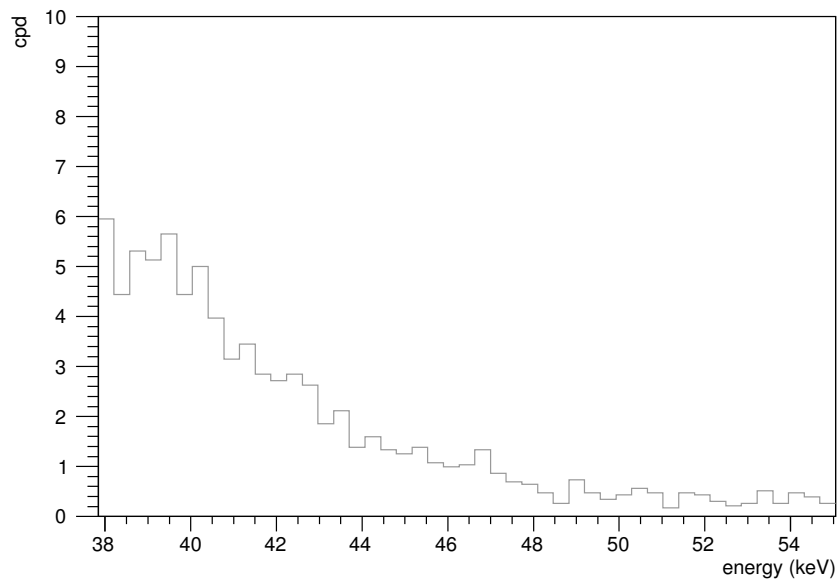
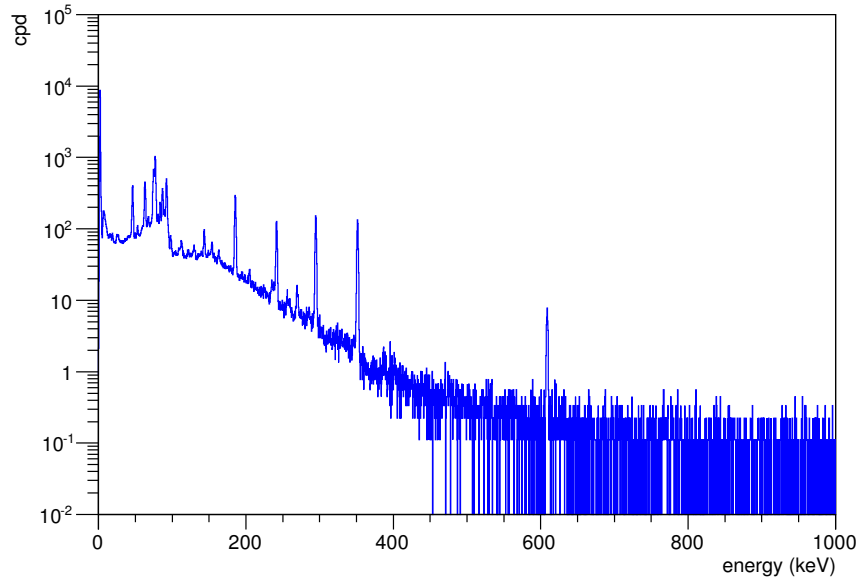
(b) ^{210}Pb window

Figure 5.2: The well detector has an acceptable background. (a) The background decreases as energy increases. (b) In the 44.5–48 keV ^{210}Pb window, the background is (10.6 ± 0.7) cpd.

5.3 Detection efficiency

The counting efficiency was measured with calibrated sources of ^{238}U and ^{232}Th [77]. Made from ore, with minimal chemical processing, the sources are in equilibrium. Each source was uniformly distributed in a silica matrix, SiO_2 , inside of a 3 mL PTFE bottle. The number of counts detected were compared to the number of decays. The detection efficiency at 46.5 keV was $(54.4 \pm 0.8)\%$. It is not to be confused with the Canberra specification of approximately 90%, which considers a point source at the bottom of the well [78]. The detection efficiencies were $(2.98 \pm 0.04)\%$ and $(14.2 \pm 0.3)\%$ for ^{214}Pb in the ^{238}U chain and ^{212}Pb in the ^{232}Th chain, respectively. See Figure 5.3 for the ^{238}U source and Figure 5.4 for the ^{232}Th source. The configuration was similar to the sample of the effluent; however, there should be a correction for the attenuation in silica. In the future, a Geant4 model will be used to calculate the attenuation due to the silica, and also due to the effluent. The attenuation could also be measured [79].



(a) Full spectrum

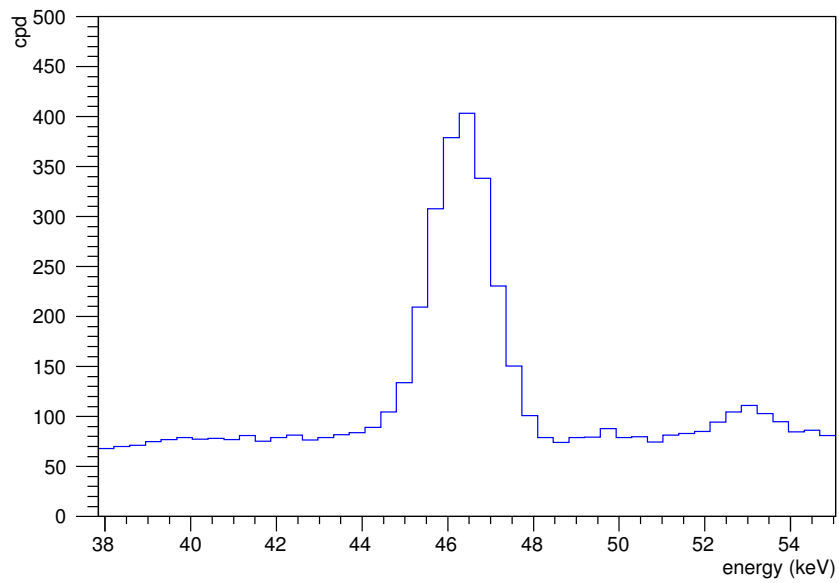
(b) ^{210}Pb

Figure 5.3: The ^{238}U calibration source was counted for 9 d. (a) The detection efficiency was determined at the following energies: 46.5, 63.3, 92.6, 143.8, 186.0, 242.0, 295.2, 351.9, and 609.3 keV. (b) The ^{210}Pb peak measured (2360 ± 20) cpd, or (1.64 ± 0.01) cpm.

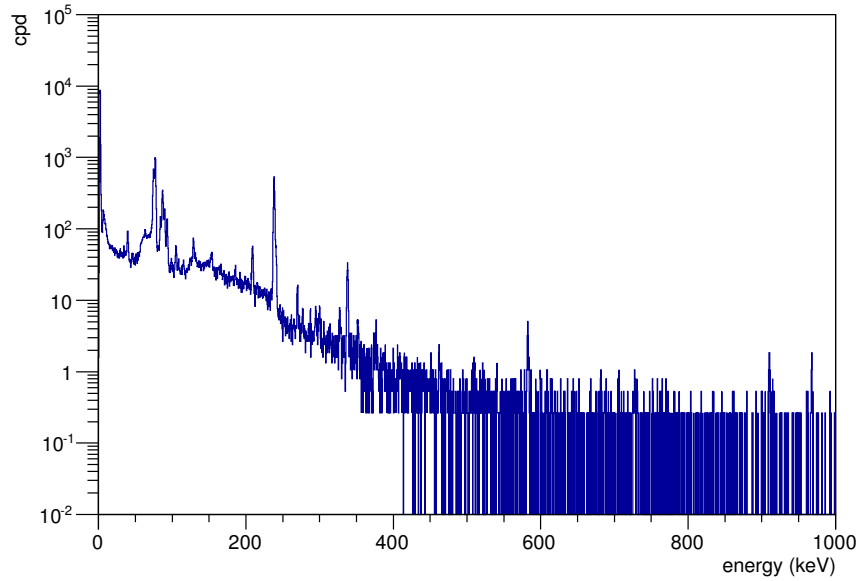


Figure 5.4: The ^{232}Th calibration source was counted for almost 4 d. The detection efficiency was determined at the following energies: 39.9, 238.6, 338.3, 538.2, 911.2, and 969.0 keV.

Chapter 6

Alpha spectrometry

Another technique was pursued for measuring ^{210}Pb from the same vaporized sample, specifically by observing the 5.304 MeV alpha from its ^{210}Po daughter. Although measuring ^{210}Pb directly in the well detector is faster and simpler, with fewer possibilities for loss or contamination, the branching fraction and detector background at 46.5 keV are disadvantages. Measuring ^{210}Po may therefore achieve better sensitivity. Storing the effluent for a month allows the collected ^{210}Pb to decay to ^{210}Po . Polonium spontaneously deposits on various metals. The radiochemistry is a simple procedure, and consists of submerging a disc into a heated solution. Low background alpha counters are used to measure the ^{210}Po on the disc.

6.1 ^{210}Po collection

There are many published procedures to collect polonium on metal discs for alpha counting, and to measure ^{210}Pb . The fact that different methods each find a high ^{210}Po collection efficiency demonstrates the robustness of the technique [80]. However, it is

not possible to assume the results of one experiment apply to even a slightly different experiment. The purpose for many of the ^{210}Po collection procedures is to estimate dose due to ^{210}Po and to track environmental processes. Samples include water, soil, food, and animals. Human urine and bone are common as well. I followed one procedure closely [81].

Nickel discs, $\frac{1}{2}$ inch in diameter, were cut from approximately 0.03 inch thick Nickel 200, pure nickel. A small hole was drilled close to the edge of each disc. Some discs were polished by hand, some with an orbital sander, and some electropolished. Finally, the discs were ultrasonically cleaned with detergent, and left to air dry. Before use, a disc was wiped with methanol. The effluent from the vaporized acrylic was transferred to a PTFE beaker, and the container that had been used to store the effluent was rinsed with three 5 mL portions of hydrochloric acid. The PTFE beaker, which had a heat resistant base, was placed on a 100°C hot plate monitored with an RTD and a multimeter. Once the sample had evaporated to near dryness, 50 mL of UPW and 100 mg of ascorbic acid were added followed by 10 mL of hydrochloric acid. For handling the disc, a length of approximately 20 cm of PTFE tape was threaded through the hole and tied with a knot. To degrease the nickel disc, it was dipped in nitric acid, then hydrochloric acid, and finally UPW. Small beakers containing approximately 10 mL were used. The disc was submerged for 2.5 h while the sample was stirred and heated to 55°C. The magnetic property of nickel on the stirrer provided the agitation. More UPW was added if the nickel disc was not completely covered. The PTFE tape could be tied to a clamp on a retort stand to keep the nickel disc in place. Direct heating on a hot plate was selected for the acrylic assay to avoid contamination due to condensing vapour from a water bath. At the

end of deposition, the disc was dipped in a small beaker of UPW and dried with boiloff N_2 gas. A Petri dish sealed with Parafilm was used to store the nickel disc before counting. The effluent was returned to an FEP bottle.

It is assumed that polonium volatilizes during acrylic vaporization, and does not volatilize during ^{210}Po collection. Again, the recovery must be measured. The temperatures are set to 500°C for vaporization, 100°C for volume reduction, and 55°C for deposition. A review on polonium in general, states that volatilization occurs at as low as 50°C [82]. Recall the study of recovery from caribou muscle and reindeer bone as a function of air temperature between $100\text{--}1000^\circ\text{C}$ [52]. Samples were heated in a furnace for 24 h, rinsed with heated acids, and ^{210}Po was collected on a silver disc. In muscle, the ^{210}Po recovery was 97% at 150°C , 60% at 200°C , and 7% at 300°C . In bone, it was 90% up to 250°C . At the end of each run, they measured the mass of the sample. The shape of the ^{210}Po recovery as a function of ashing temperature, matched the shape of the final mass as a function of ashing temperature. It was suggested that perhaps polonium is trapped within the matrix and cannot volatilize until the sample itself volatilizes. This relationship was not observed for ^{137}Cs . They also investigated the time scale of volatilization by running samples for 1, 2, 4, 8, 24, 48, 72, and 144 h at 200, 250, and 300°C . Any ^{210}Po volatilization occurred in the first hour. In what seems like a similar experiment, the ^{210}Po recovery after 16 h in a 500°C furnace was 13% from a rat kidney and 7% from a rat femur [83]. The difference between this study and the previous study is the exposure. The rat had been injected with ^{210}Po and killed 4 h later, whereas the source of ^{210}Po for the caribou and reindeer was a lifetime of ingesting ^{222}Rn daughters from the air that had accumulated on lichen. According to a review of ^{210}Po collection, the temperature

should be kept below 100°C [80].

It is of interest to optimize ^{210}Po collection, and there are many factors to consider. Of the metals investigated for spontaneous deposition of polonium, the most common are nickel and silver, and copper. Although nickel has been shown to have higher collection efficiency [84, 85], there are advantages to silver and it is favoured [80]. The use of silver may minimize contamination of the alpha counter; however, further investigation is required. Discs with deposited polonium were heated to $>250^\circ\text{C}$ and it was found that silver had less loss compared to nickel [85].

Co-deposition of ^{210}Pb and ^{210}Bi can complicate the calculation of the ^{210}Po activity. Copper and nickel are understood to have co-deposition. There is some indication that silver may have less co-deposition [86], but reports are contradictory [80]. Performing several depositions to study the activity over time could provide an indication of co-deposition. Separation of ^{210}Po before deposition, for example by co-precipitation or with resin, is another option. Tracers can be used to determine the collection efficiency. Typical isotopes used are ^{208}Po and ^{209}Po . The half-life of ^{208}Po is 2.898 y and the energy of the alpha is 5.1115 MeV. The half-life of ^{209}Po is 102 y and it alpha decays 99.52% of the time. There are two main alphas, 4.883 MeV with 79% and 4.885 MeV with 20% [42]. The longer half-life and that the alphas are further separated from the 5.304 33 MeV alpha from ^{210}Po are advantages to ^{209}Po [80]. Either ^{208}Po or ^{209}Po may be used, or both [85]. Perhaps ^{208}Po could be added before volume reduction, and ^{209}Po before deposition. A source containing all three of ^{210}Pb , ^{210}Bi , and ^{210}Po in equilibrium has also been used [53, 84], as well as isolated ^{210}Po [87].

Discs are prepared from sheets of metal. Collection efficiency improves with area

of the disc, as demonstrated with a 1.5 inch diameter disc and a 1 inch diameter disc [53]. It may be preferred, however, to have increased alpha counting efficiency with a small disc. The efficiency can be improved by a factor of 2 by having ^{210}Po deposit on just one side of the disc instead of both. A PTFE coating is suggested [80]. An investigation of polyethylene melted to nickel discs found that just 1–5% of the total activity was lost to the coated side of the disc [53]. Acid resistant paint was mentioned [81], and was incorporated during the first attempts of ^{210}Po collection for the acrylic assay. A product of that generic description of heavy duty acid-resistant coating was purchased from McMaster-Carr and applied to nickel discs. The paint did not stand up to aqua regia, and neither did the nickel. The paint became separated from the disc, the disc was corroded, and the effluent turned green. Not only was that disc damaged, but the fumes also damaged all of the other polished discs that were sitting in the fume hood. The paint has not been used since, although it may be suitable for the hydrochloric acid in the revised procedure. Another option is to have ^{210}Po deposit on both sides of the disc and count both sides. Currently, only one side of the disc has been polished. The recommended cleaning procedure for silver discs is polishing with a slurry of aluminum oxide, washing with water, and wiping with alcohol [80].

Deposition occurs from a solution of hydrochloric acid. The volume should be minimized for improved collection and is typically around 10 mL [80]. Concentrations of 0.1–12 M have been used, and 0.1–0.5 M is recommended [80]. Testing the pH is simplest, and the solution can be adjusted with sodium hydroxide if necessary. For $\text{pH} < 0$ corrosion of the disc degraded alpha resolution, and for $\text{pH} > 1$ ^{210}Po adsorbed to the container [87]. Polonium is known to stick to glass [82], and a PTFE container

has been suggested [87]. The walls can be sprayed frequently with UPW [52] or hydrochloric acid [53]. Ascorbic acid, 50–200 mg, is used to prevent interference from iron [80]. Hydroxylammonium chloride can be used instead, but ascorbic acid is more effective. Stirring also improves the collection efficiency. Agitation can be achieved by spinning the disc, or with a stir bar and a stirrer. One group mentioned 400 rpm [53], while another suggested as fast as possible without splashing [81]. Bubbling air, or another gas, through the solution is another option [85]. Temperatures between 60–100°C, and even room temperature [84], have been used. The conclusion is that 80–90°C is best [80]. The submersion time ranges from 1.5 h to 24 h, with a mean of about 5 h; overall 2–3 h is suggested [80]. When ^{210}Po collection is complete, the disc is rinsed with water. There are various examples of drying in air [53], on a hot plate [81], or in an oven [87], and also cleaning with ethanol [81] or acetone [85]. Overall, spontaneous deposition of ^{210}Po onto metal discs produces a good sample for alpha spectrometry. The sensitivity is at the level of 10^{-18} g ^{210}Po [80]. It depends on how the detection level is determined, but there is a report of 10^{-23} g/g for ^{210}Bi and 10^{-23} g/g for ^{210}Po [54]. Even 50 years ago, a detection limit of 4×10^{-18} g ^{210}Po was published [53].

Based on this review, I recommend the following changes to the procedure currently used for ^{210}Po collection, and emphasize that the collection efficiency cannot be estimated from the literature. Co-deposition of ^{210}Pb and ^{210}Bi with ^{210}Po must be considered. A ^{209}Po tracer should be used. There should be a second deposition after another 30 d to study the activity of the effluent over time. Both sides of silver discs should be polished with aluminum oxide, before being ultrasonically cleaned with detergent and wiped with methanol. A PTFE stir rod might improve mixing of

the solution, but should be kept small to minimize the volume of the solution. A hole in the disc would no longer be necessary. Coating one side of the disc with PTFE would be beneficial. Although the 2 M concentration of hydrochloric acid is a bit high, it should not be adjusted to make a large dilute volume without investigation. The temperature should be monitored more accurately, since the reading from the hot plate or by an RTD making contact with the hot plate gives large fluctuations. Every 30 min, the walls should be washed with hydrochloric acid. A deposition of 3 h at 85°C is suggested.

6.2 Low background alpha counter

Two low background 450 mm² ORTEC ULTRA-AS ion-implanted-silicon detectors were purchased by Queen's University for this measurement. The Alpha Ensemble can hold four Alpha Duos for a total of eight counters. Since there is currently one Alpha Duo, with Alpha 1 and Alpha 2, blank panels cover the unoccupied spaces. The pressure is common to both chambers, and is controlled between 10 mTorr and 20 Torr. A pressure of 200 mTorr has been used for counting. A counter can accept 13–51 mm diameter samples, and the sample-to-detector spacing is 4–44 mm, in increments of 4 mm. Battery-biased sample holders keep the positively charged recoiling nuclei from contaminating the detector. Note, however, that recoil protection does not prevent contamination due to volatilization. It is suggested to leave the disc in air for 2 d before counting [80]. This may help by allowing an oxide to form. It is inevitable that the counters will acquire some contamination over time. When not in use, the chambers are kept at vacuum and with caps over the detectors. The history is carefully recorded. In addition to the air exposure, the log is used to record the sample

description, the orientation on the holder, and the distance between the sample and the detector. Sample preparation is also described in detail. The data are saved in 10 min intervals.

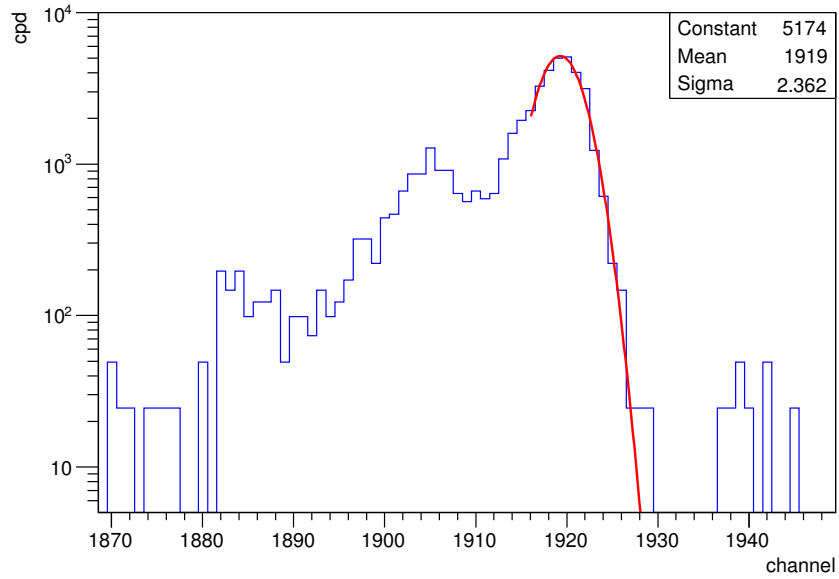
6.3 Energy calibration and resolution

An encapsulated, collimated ^{241}Am source was used to calibrate the detectors.¹ In addition to the alpha used for the calibration, another two alphas from ^{241}Am are observed. See Table 6.1 [42]. The channel range was selected manually and a Gaussian was fit to the largest peak. See Figure 6.1. Instead, the ^{241}Am spectrum could be fit with a composite fit function made of three Gaussians. To determine the thickness of the dead layer, the ^{241}Am source was placed directly under the detector, and then at an angle. See Figure 6.2. The energy calibration and resolution remained practically the same and it is concluded that the effect of the dead layer is negligible.

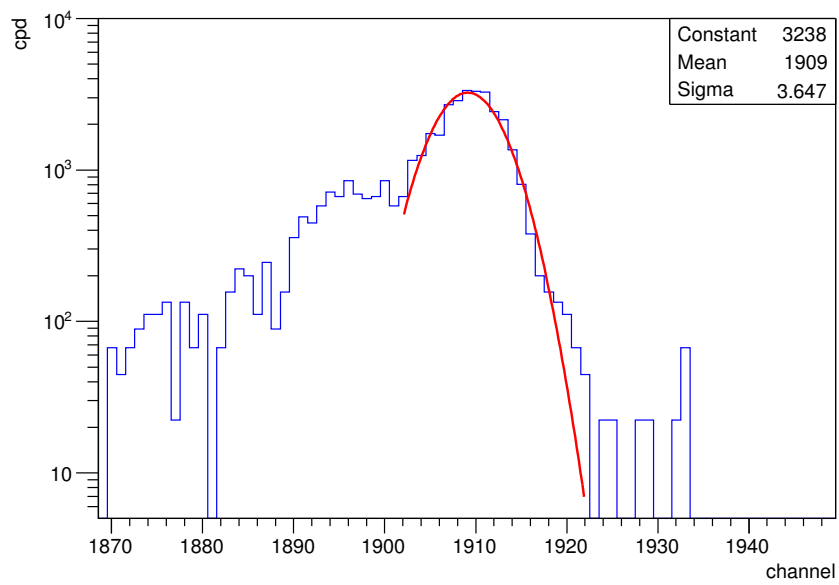
Table 6.1: ^{241}Am for calibration

alpha energy (MeV)	branching fraction (%)
5.388	1.66
5.4428	13.1
5.4856	84.8

¹Thanks to Peter Skensved and Peter Rau for helping to set up the alpha counters and taking the ^{241}Am data.



(a) Alpha 1



(b) Alpha 2

Figure 6.1: Gaussian fit of the 5.4856 MeV alpha from ^{241}Am to determine the energy calibration and resolution.

- (a) Alpha 1 finds the peak at channel 1919, with a FWHM of 16 keV.
- (b) Alpha 2 finds the peak at channel 1909, with a FWHM of 25 keV.

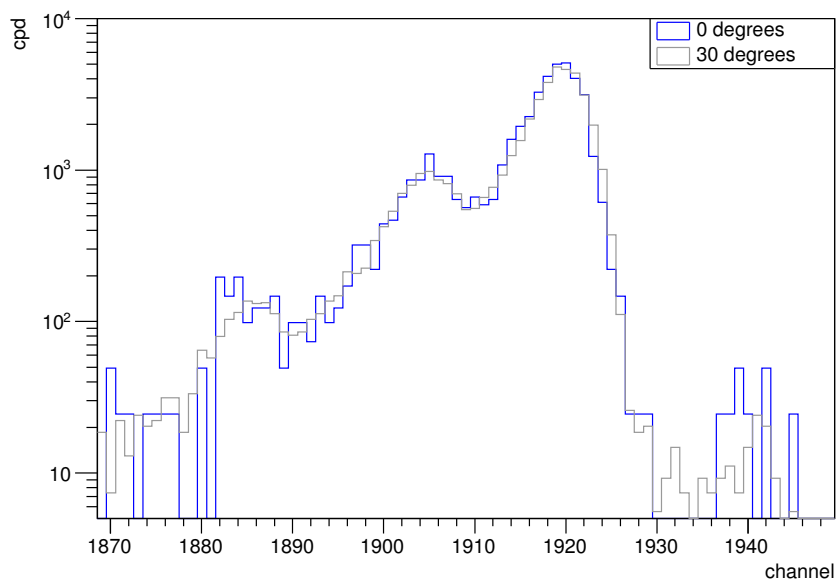
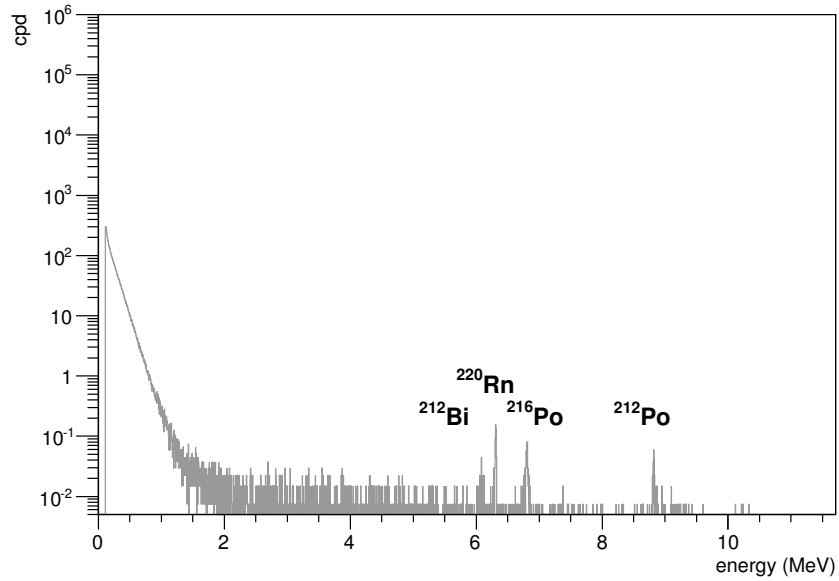


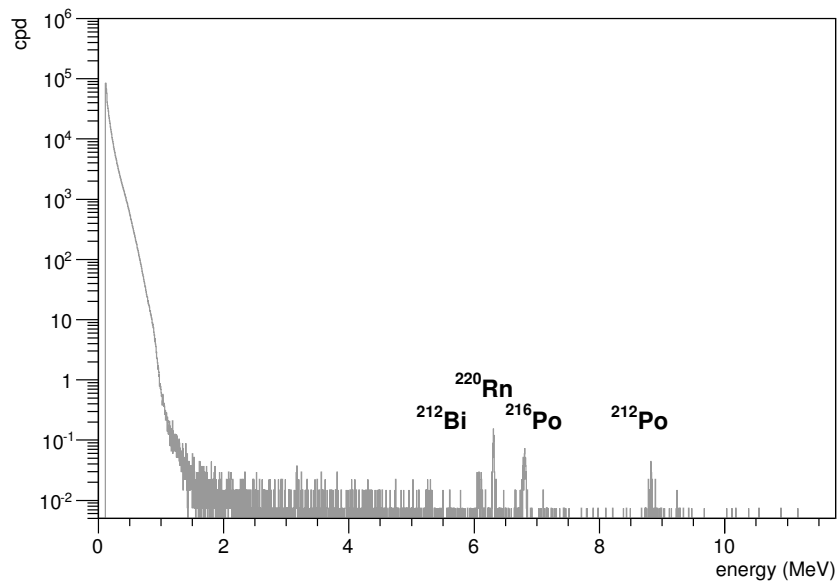
Figure 6.2: The dead layer has a minor effect. The ^{241}Am source was placed under Alpha 1, at 0° and 30° . At 30° , the 5.4856 MeV peak is at channel 1920, and the resolution is 17 keV ($\sigma = 2.48$).

6.4 Background

To quantify the backgrounds, the empty detectors collected data for almost 5 months. See Figure 6.3. Four small peaks are observed, in both counters, and can be explained by the ^{232}Th chain starting at ^{220}Rn . See Figure 6.4. It is possible that there is some radium or thorium in the materials that make up the counter. A window for the ^{210}Po peak was selected as 3.5–5.35 MeV to account for broadening due to surface effects. With more experience counting ^{210}Po , this window could be narrowed.



(a) Alpha 1

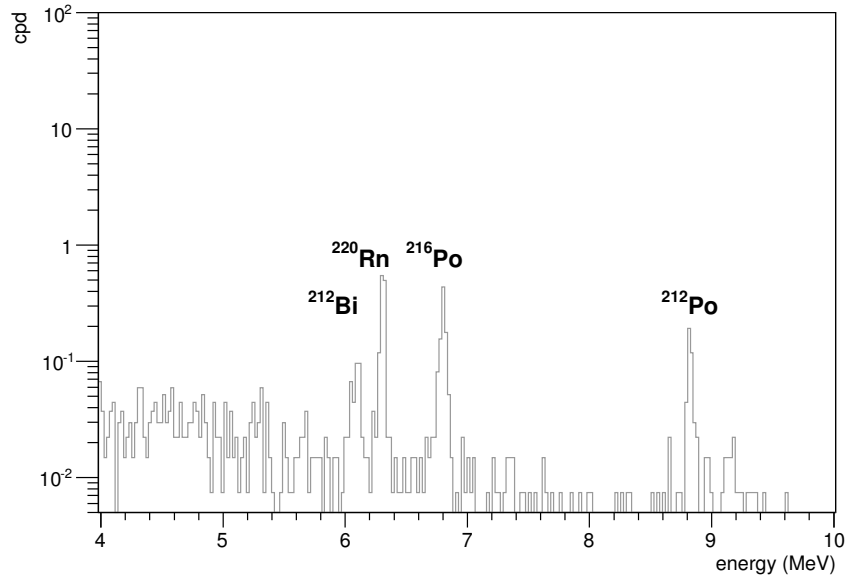


(b) Alpha 2

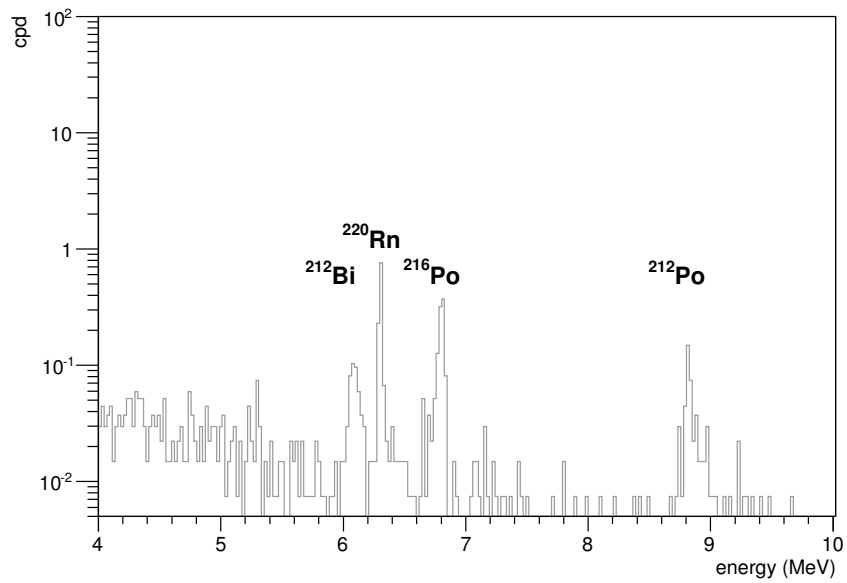
Figure 6.3: A new alpha counter is guaranteed ≤ 24 cpd at 3–8 MeV, and can be as low as 6 cpd [88]. The ^{210}Po window is 3.5–5.35 MeV.

(a) Alpha 1: (7.1 ± 0.2) cpd at 3–8 MeV, and (2.78 ± 0.14) cpd for ^{210}Po .

(b) Alpha 2: (6.7 ± 0.2) cpd at 3–8 MeV, and (2.49 ± 0.14) cpd for ^{210}Po .



(a) Alpha 1



(b) Alpha 2

Figure 6.4: The peaks in the empty alpha counters are attributed to alphas at 6.05 MeV and 6.09 MeV from ^{212}Bi , 6.29 MeV from ^{220}Rn , 6.78 MeV from ^{216}Po , and 8.78 MeV from ^{212}Po [42].

6.5 Counting efficiency

Due to geometry, the efficiency of the alpha counter is $(15 \pm 2) \%$. First of all, 50% of the ^{210}Po will be on the bottom of the nickel disc. Of the activity on the top, 50% of the alphas will go in the downwards direction away from the detector. For the alphas that go upwards, there is a solid angle based on the 8 mm separation between the nickel disc and the detector. From the given area of the detector, 450 mm^2 , the radius is 12 mm. The nickel discs have a $\frac{1}{2}$ inch diameter, or a 6.35 mm radius. A simulation was used to determine the solid angle by generating events from the disc and finding what events made contact with the detector. It was assumed that the sample and detector were circular and coaxial, and that the source of alphas was homogeneous. One million events were generated on a square in the xy plane. Only the events within the radius of the disc were accepted, and the components of this location vector were found. For each event, an upwards direction was assigned. It was calculated where the direction vector intersected with the plane of the detector, 8 mm away in the z-direction. The direction vector and the event location vector were combined to find the total vector. An event was detected if the magnitude of the total vector was less than the radius of the detector. See Figure 6.5 for the events on the nickel disc and detector. The ratio of the number of events at the detector to the number of events generated on the disc was found. An uncertainty of 1 mm was assumed for each of the detector radius, the disc radius, and the separation. The uncertainty on the solid angle efficiency is from the range of possibilities. The worst possible solid angle efficiency, 52%, involves a small detector, a large disc, and a large separation. The best, 68%, involves a large detector, a small disc, and a small separation. The statistical uncertainty is negligible. The solid angle efficiency

is $(60 \pm 8)\%$. The efficiency of detecting an alpha that reaches the detector should be measured with a source of known activity.

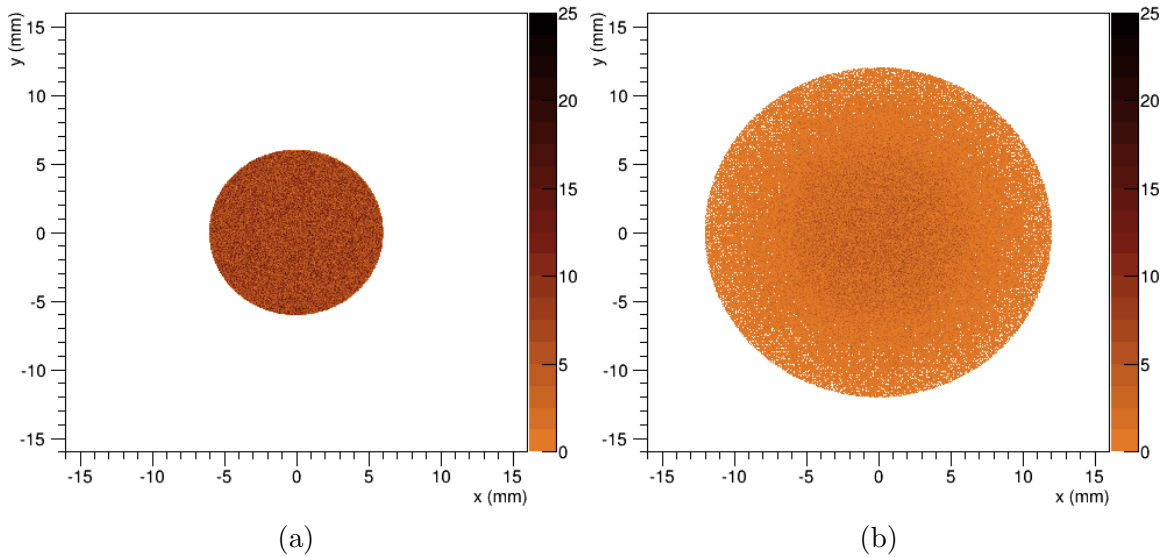


Figure 6.5: The solid angle of the alpha counter was calculated by a simulation that sent events from the disc upwards to the detector. (a) Alphas were uniformly distributed on the $\frac{1}{2}$ inch disc. (b) The 450 mm^2 detector is 8 mm from the disc.

Chapter 7

Recovery efficiency

Before vaporizing a sample of the DEAP-3600 AV acrylic, the losses during vaporization, rinsing, and ^{210}Po collection were determined. A spike with ^{210}Pb from a ^{222}Rn source was measured in both the well detector and the alpha counter. Another spike with stable lead was analyzed by ICP-MS. SNO measured only 4% loss from vaporization and rinsing using spikes of thorium and radium; recall that the rinse was nitric acid and hydrofluoric acid instead of aqua regia [69]. The recovery efficiency of lead, and later including polonium, was measured for this acrylic assay.

7.1 ^{210}Pb from ^{222}Rn source

A spike should be as similar as possible to the contamination in the acrylic used for the DEAP-3600 AV. From a calculated amount of ^{222}Rn , ^{210}Pb was added to acrylic. This allowed for a measurement of the overall recovery efficiency of the system, which involves vaporization, rinsing, ^{210}Po collection, and counting. A ^{222}Rn source was used with an acrylic chamber. The ^{222}Rn source, RN-1025 from Pylon Electronics Inc., has

an activity of 526.545 kBq equilibrium or 66 239.419 mBq/min continuously available from ^{226}Ra powder. According to the manual, the ^{226}Ra is contained by filters [89]. The 106 cm^3 aluminum housing is surrounded by valves, and there is a drying column at the inlet. External in-line filters should be changed regularly. Operating ranges are 0–3 atm, 0–10 L/min at 1 atm and ambient pressure, and 0–95 % relative humidity. In terms of radiation safety a beta-gamma survey meter was on hand; however, there is a delay for betas and gammas to come from ^{222}Rn daughters. The chamber was made from an acrylic tube from McMaster-Carr that was cut to a length of 15 cm. Acrylic cement, Weld-On 42 for example, was used to attach an acrylic disc to the end of the chamber. At the other end, an aluminum clamp with an O-ring made a seal. After ^{222}Rn was transferred from the source to the chamber, the chamber was sealed while ^{222}Rn decayed to ^{210}Pb . The chamber was brought to SNOLAB for vaporization, rinsing, and counting in the well detector. The effluent was left for about a month for ^{210}Pb to decay to ^{210}Po . The ^{210}Po was collected and the sample was measured in the alpha counter at Queen's. The spike was designed to have approximately 100 cpd ^{210}Pb in the well detector and 100 cpd ^{210}Po in the alpha counter.

A series of decays are described by the Bateman equations [90]. These were used for the decay of ^{222}Rn to ^{210}Pb , and for the decay of ^{210}Pb to ^{210}Po . The half-lives are shown in Tables 7.1 and 7.2, respectively [42]. From the known initial activity, N_1 , the activity of the n^{th} daughter, A_n , is determined. The uncertainty in time, t , is negligible. The prime indicates that $i \neq m$ for the product in the denominator.

$$A_n = N_1 \sum_{i=1}^n c_i e^{-\lambda_i t} \quad (7.1)$$

$$c_m = \frac{\prod_{i=1}^n \lambda_i}{\prod_{i=1}^n (\lambda_i - \lambda_m)} \quad (7.2)$$

Table 7.1: ^{222}Rn to ^{210}Pb

Label	Nuclide	$t_{1/2}$
1	^{222}Rn	3.8235 d
2	^{218}Po	3.098 min
3	^{214}Pb	26.8 min
4	^{214}Bi	19.9 min
5	^{214}Po	164.3 μs
6	^{210}Pb	22.20 y

Table 7.2: ^{210}Pb to ^{210}Po

Label	Nuclide	$t_{1/2}$
1	^{210}Pb	22.20 y
2	^{210}Bi	5.012 d
3	^{210}Po	138.376 d

7.1.1 Successful spike

The setup consisted of the ^{222}Rn source, a liquid nitrogen cooled stainless steel coil as a trap, two Lucas cells, and an empty acrylic chamber. See Figure 7.1. A Lucas cell is an evacuated acrylic container coated with scintillating $\text{ZnS}(\text{Ag})$ paint used for measuring radon by counting with a PMT. Instead of calculating the ^{222}Rn activity from the calibrated source, it was measured. A counting time of 10 min was used and after 3 h, at which point the alpha-emitting daughters, ^{218}Po and ^{214}Po , are approximately in transient equilibrium with the parent, ^{222}Rn . From the count rate, the ^{222}Rn activity is found by dividing by three, since there are three alphas, and

correcting for the detection efficiency, $(74 \pm 7) \%$ [91].

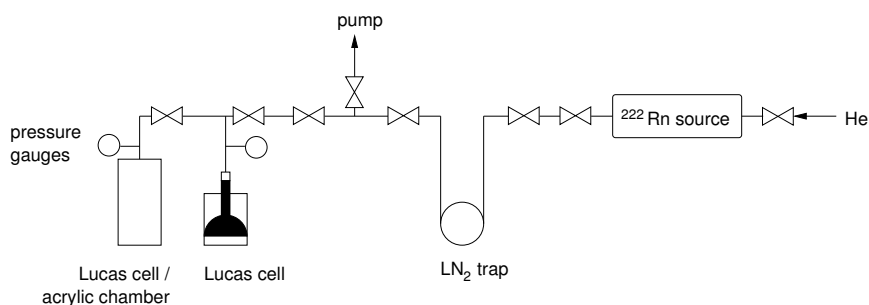


Figure 7.1: A measured amount of ^{222}Rn was transferred to an evacuated acrylic chamber. Lucas cells measured ^{222}Rn to understand the available volumes during free expansion. The acrylic chamber was sealed for 2 weeks while ^{222}Rn decayed to ^{210}Pb . After vaporization, rinsing, and ^{210}Po collection, the recovery efficiency of lead was determined [56].

The procedure begins by pumping out the Lucas cells for 2 h and measuring the backgrounds. This was done the day before the spike. In all cases, the backgrounds were <1 cps and negligible. Upon reattaching the Lucas cells to the setup, they were pumped out for another 30 min. The source was purged with helium from a gas cylinder. The exhaust line, during the purge and also during pumping, was tubing in a vent to outside. The source was then closed and left to regenerate for 2 h. After 1.5 h, the trap was evacuated and cooled with LN_2 for 30 min. Any helium in the trap would not freeze. The LN_2 was contained in a beaker insulated with bubble wrap. Although the trapping efficiency can be improved, by loading the tubing with brass wool for example [92], this trap was empty. A valve at the source was opened and the ^{222}Rn gas moved from the source to the trap by free expansion for 10 min. The source can tolerate a pressure drop of 6 psi with $0.8 \mu\text{m}$ filters, and 4 psi without filters [89]. It is important not to leave the source at vacuum, and it was returned to atmospheric

pressure from a plastic bag filled with helium. Another 10 min were allowed for the ^{222}Rn to stop in the trap. The trap was then opened to the Lucas cell, and the pressure was -16.5 inch Hg. The uncertainty was estimated to be 0.5 inch Hg from reading the pressure gauge. While keeping LN_2 on the trap, the system was slowly evacuated to the low pressure necessary to use a Lucas cell. The gauge had a minimum of -30 inch Hg, therefore to have a measurable pressure, -28.5 inch Hg was used. The trap was warmed with a heat gun until it felt like room temperature to touch, which took about 3 min. The pressure was monitored while warming the isolated trap from LN_2 temperature. For another 10 min, the ^{222}Rn redistributed and the pressure was -25.5 inch Hg. The Lucas cell was removed and counted. To understand the transfer from the Lucas cell to the acrylic chamber through the connecting tubing, a transfer was first completed between two Lucas cells. The spiked Lucas cell was opened to another Lucas cell attached where the acrylic chamber would be. The pressure was -29.5 inch Hg. Having the same volume, the Lucas cells obtain equal amounts of ^{222}Rn . The activity in the tubing was determined as the difference between the initial amount and the amount in both Lucas cells. The acrylic chamber was pumped out for 30 min, and one Lucas cell was then opened to the evacuated chamber. The pressure was off the scale, < -30 inch Hg. The chamber was isolated and left for ^{222}Rn to decay to ^{210}Pb . The rest of the line and the Lucas cells were evacuated to minimize contamination from ^{222}Rn . Each Lucas cell was pumped out for 30 min, and counted to confirm the activity was removed. After 2 weeks, the chamber was opened to the room. In the approximately 3 min that it was opened, it is expected that the small amount of remaining ^{222}Rn would have diffused out and that the ^{210}Pb remained. The chamber was closed using a Swagelok cap. The acrylic chamber was vaporized

and rinsed. The effluent was counted directly in the well detector, and was used later for alpha counting.

To calculate the expected ^{222}Rn activity in the acrylic sample, the volumes of the Lucas cells, the tubing, and the acrylic chamber were needed. The volume of a Lucas cell is $(15.5 \pm 0.5) \text{ cm}^3$ [93]. The volume of the tubing was calculated to be $(12 \pm 3) \text{ cm}^3$ by estimating the diameter and measuring the length of every piece of tubing, valve, and fitting. The $\frac{1}{4}$ inch Swagelok tubing was estimated to have a wall thickness of $(0.049 \pm 0.015) \text{ in}$. The $\frac{1}{4}$ inch pieces from Swagelok were given an uncertainty of $\frac{1}{32}$ inch, whereas all other types of $\frac{1}{4}$ inch pieces were given an uncertainty of $\frac{1}{16}$ inch. When measuring a length with a ruler, the uncertainty was 0.1 cm. The volume of the tubing was confirmed using a Lucas cell filled with air. The fitting for the other Lucas cell had been capped off and the line was evacuated. A Lucas cell at atmospheric pressure, 0.0 inch Hg on the gauge, was attached to the evacuated system, -30.0 inch Hg, and the volume of the tubing was determined by the pressure change. From three trials, the average was $(-13.9 \pm 0.3) \text{ inch Hg}$. The pressure scale was shifted to set atmospheric pressure to 30 inch Hg instead of 0 inch Hg. The initial pressure and volume were $(30.0 \pm 0.5) \text{ inch Hg}$ in the Lucas cell. The final pressure and volume were $(16.1 \pm 0.3) \text{ inch Hg}$ in the Lucas cell and tubing. By the ideal gas law,

$$T = L \left(\frac{P_1}{P_2} - 1 \right) \quad (7.3)$$

where T is the volume of the tubing, L is the volume of the Lucas cell, P_1 is the initial pressure, and P_2 is the final pressure. The volume of the tubing was determined to be $(13 \pm 1) \text{ cm}^3$. The measurement was repeated with a Lucas cell at atmospheric

pressure, the evacuated tubing and an evacuated Lucas cell. In this case,

$$T = L \left(\frac{P1}{P2} - 2 \right) \quad (7.4)$$

and the volume of the tubing was measured to be $(13 \pm 2) \text{ cm}^3$. Although it was a simple task, it was satisfying that the three methods agreed. The measurement with the smallest uncertainty, $(13 \pm 1) \text{ cm}^3$, was used as the volume of the tubing. The volume of the acrylic chamber was calculated to be $(170 \pm 20) \text{ cm}^3$. The cylindrical chamber had a 2 inch outer diameter and a $\frac{1}{4}$ inch wall thickness with an uncertainty of 15%. The diameter of the chamber was $(3.8 \pm 0.2) \text{ cm}$. The height of the chamber was measured with a ruler to be $(15.0 \pm 0.1) \text{ cm}$.

Lucas cell measurements used to calculate the ^{222}Rn activity are shown in Table 7.3. The spiked Lucas cell, called Lucas cell 2, was measured to have $(330 \pm 40) \text{ Bq}$ ^{222}Rn before it was opened to the empty Lucas cell 1. The total volume was the sum of two Lucas cells and the tubing, $(44 \pm 1) \text{ cm}^3$. Each Lucas cell was expected to take $(35 \pm 2) \%$ or $(120 \pm 20) \text{ Bq}$, which agrees with the $(100 \pm 10) \text{ Bq}$ and $(110 \pm 10) \text{ Bq}$ that were measured for the Lucas cells, respectively. The decay after 3 h has no effect considering the uncertainty on the activity. The tubing would have had the remaining $(30 \pm 2) \%$ or $(100 \pm 10) \text{ Bq}$. Lucas cell 2, with $(110 \pm 10) \text{ Bq}$, was then attached to the evacuated acrylic chamber. The total volume was the sum of the Lucas cell, the tubing, and the chamber, $(200 \pm 20) \text{ cm}^3$. The expected activity for the Lucas cell after transfer, $(7.8 \pm 0.8) \%$ or $(9 \pm 1) \text{ Bq}$, was consistent with the measured $(12 \pm 2) \text{ Bq}$. The tubing should have had $(6.5 \pm 0.8) \%$ of the activity, or $(7 \pm 1) \text{ Bq}$. The remaining $(90 \pm 10) \%$ would have gone to the chamber. The activity in the acrylic chamber was therefore $(90 \pm 20) \text{ Bq}$.

Table 7.3: Lucas cell ^{222}Rn results from spike

description	Lucas cell	count rate (cps)	^{222}Rn (Bq)
spike from trap	2	730 ± 60	330 ± 40
Lucas cell transfer	1	220 ± 20	100 ± 10
	2	250 ± 20	110 ± 10
acrylic chamber transfer	2	28 ± 2	12 ± 2

In the 12 d that the chamber was sealed, 90% of ^{222}Rn would have decayed. It was calculated that (90 ± 20) Bq ^{222}Rn produced $(4.1 \pm 0.8) \times 10^7$ atoms ^{210}Pb . The sample was vaporized, rinsed, and the volume was reduced for counting in the well detector. Considering the branching fraction of 4.25%, the (3500 ± 700) cpd ^{210}Pb gives a gamma rate of (150 ± 30) cpd at 46.5 keV. With the detection efficiency at that energy, $(54.4 \pm 0.8)\%$, (80 ± 20) cpd were expected in the well detector.

The effluent was left for 36 d for the $(4.1 \pm 0.8) \times 10^7$ atoms ^{210}Pb to decay to ^{210}Po at (460 ± 90) cpd. Half of the alphas are on the top side of the nickel disc, (230 ± 50) cpd, and half of those go towards the detector, (120 ± 20) cpd. The solid angle is $(60 \pm 8)\%$, therefore the expected alpha rate was (70 ± 20) cpd.

7.1.2 Lucas cell counting

The use of Lucas cells to measure ^{222}Rn was carefully studied before accepting a spiked acrylic sample for vaporization and rinsing. Two counters were used: Counter A refers to the PMT on the left in the SNO radon emanation lab, and Counter B refers to the PMT on the right. The counters were compared using a ^{222}Rn -spiked Lucas cell by alternating 10 min of counting in Counter A and Counter B over 24 h. The procedure

for loading the Lucas cell with ^{222}Rn was similar to that described above, and will be described only briefly. After pumping out the Lucas cell for 2 h, the background was measured to be negligible. The Lucas cell was pumped out for another 30 min. The source was then purged with helium, and then left to regenerate for 2.5 h. The stainless steel trap was evacuated and cooled with LN_2 for 30 min. The source was opened to the trap for 10 min. The trap was closed for another 10 min. The trap was opened to the Lucas cell, and the pressure was -16.5 inch Hg. The trap was slowly evacuated to -28.5 inch Hg, and then warmed with a heat gun. After waiting 10 min, the pressure had increased to -25.0 inch Hg. The Lucas cell was removed and counting began.

The two counters used to measure ^{222}Rn with Lucas cells are equivalent, and the results were as expected. See Figure 7.2. Although equilibrium is not reached until 4.4 h (264 min), our decision to count a Lucas cell after 3 h is justified. At that time, the ratio of the ^{214}Po activity to the ^{222}Rn activity is 95%. See Figure 7.3 for the spectra immediately after the spike and after 3 h. The uncertainty on the count rate can also be determined. The statistical uncertainty from the number of counts is negligible. The variation between Counter A and Counter B is a sampling of some systematic uncertainty. See Figure 7.4 for the distribution of the percent difference. Sources of systematic uncertainty could include changes in the gain because of frequently dialing up and down the high voltage, temperature changes over 24 h, magnetic fields from surrounding equipment turning on and off, or the coupling between the Lucas cell and the PMT. The mean difference of 3% between the counters samples some of these systematics, but not all. A total uncertainty of 8% on the count rate, gives a good fit between the theory and data from Counter A.

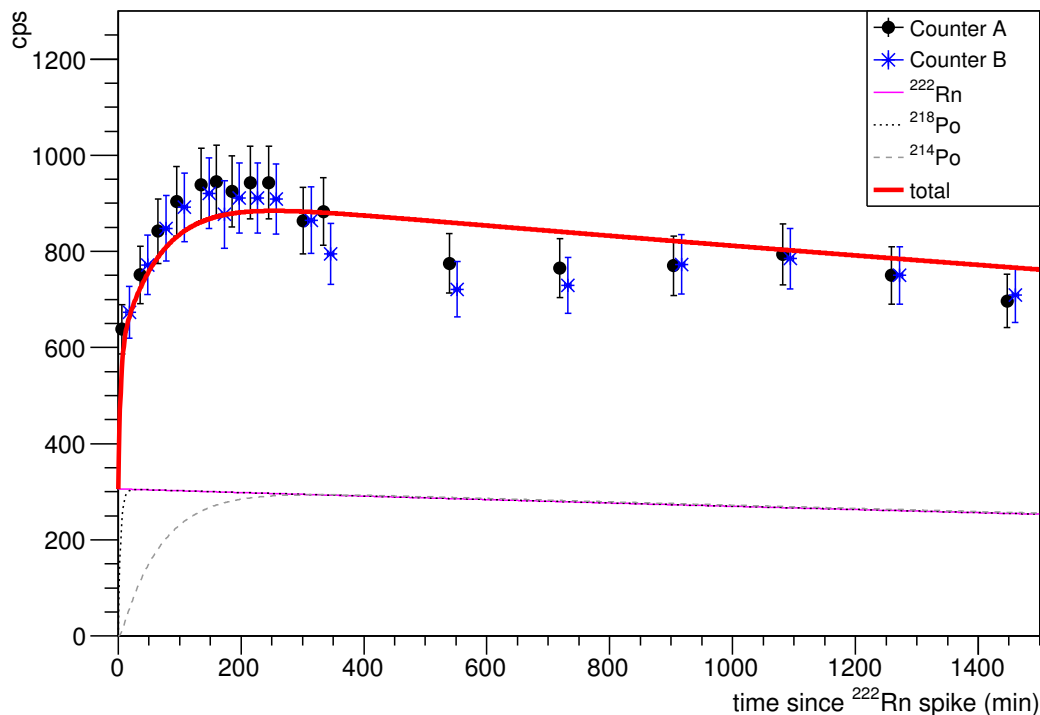
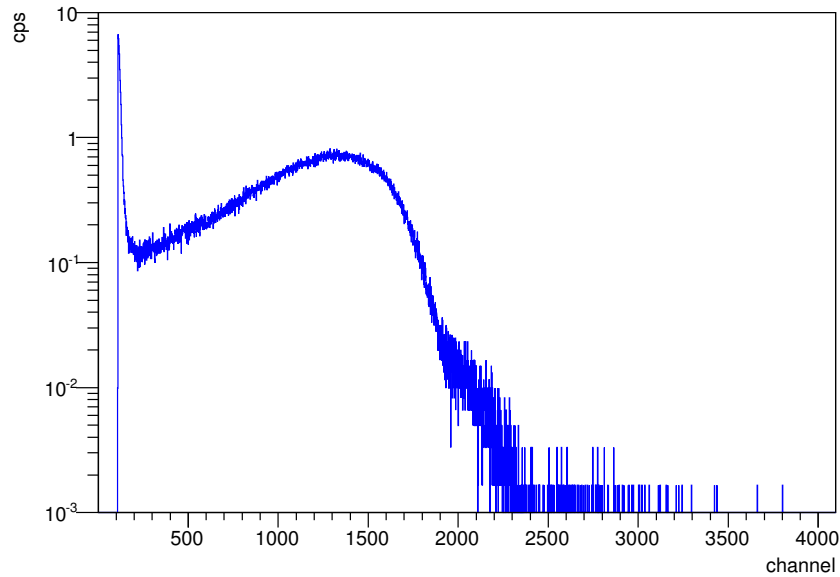
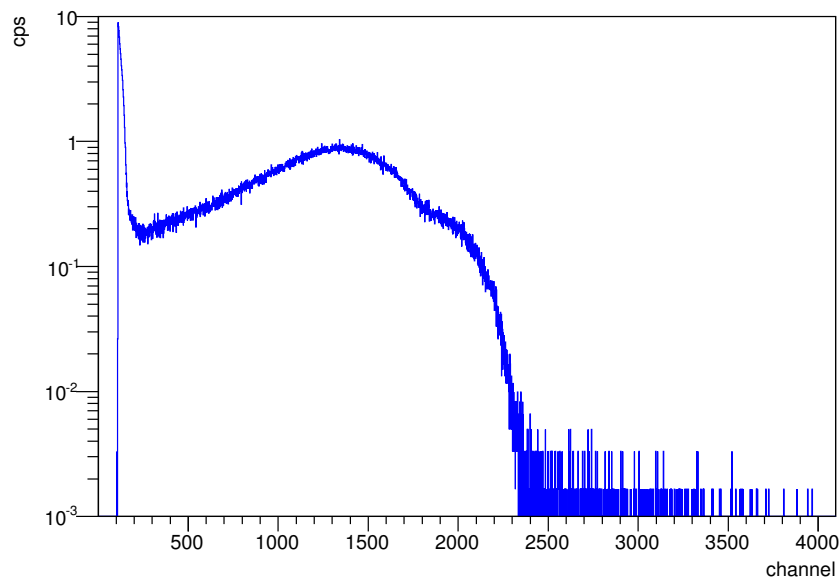


Figure 7.2: Results from the two Lucas cell counters agreed with theory. The calculated curves for ²²²Rn, ²¹⁸Po, and ²¹⁴Po were summed for the total activity. The initial amount of ²²²Rn was adjusted for the best fit between the total activity and the data. Only Counter A was used for the fit; however, the two counters are the same. The uncertainties on the count rate were estimated as 8% to give an acceptable fit ($\chi^2 = 12$, $df = 15$).



(a)



(b)

Figure 7.3: An alpha causes scintillation in the Lucas cell that is measured by a PMT. This system has not been calibrated. (a) Immediately after the spike, the 5.4851 MeV alphas from ^{222}Rn are observed. (b) After 3 h, the average energy has increased due to the alphas from ^{218}Po at 6.0011 MeV and from ^{214}Po at 7.686 01 MeV [42].

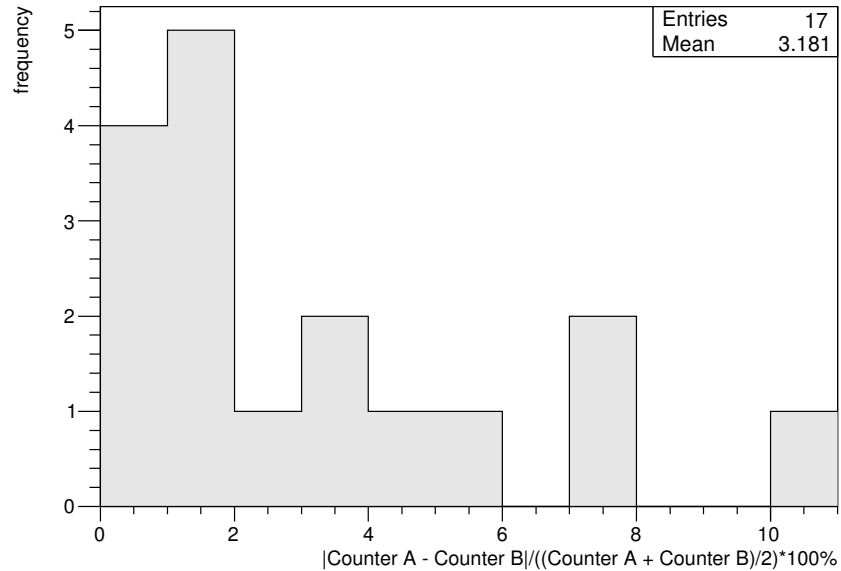


Figure 7.4: The distribution of the difference between Counter A and Counter B over 24 h had a mean of 3%.

Adjustments were made in hardware to make the counters the same. For example, the gain of Counter B was changed to increase the peak position to be the same as Counter A. Counter B was also set to 4096 channels like Counter A, instead of 8192. The hardware for Counter B is limited. Although the electronics noise is easy to distinguish in Counter A, the low-level discriminator (LLD) in Counter B is set at 113 and cannot be changed. A cut at channel 200 is appropriate for Counter A, and is also used for Counter B. Actually, the LLD in Counter A was increased from 0 to 100 in an attempt to minimize the dead time. The reasonable dead time of approximately 0.5% from Counter A is assumed for both counters since Counter B always incorrectly shows 100% dead time.

7.1.3 Previous attempts

In addition to the successful spike, 11 spikes were prepared and many others were attempted.¹ Leaks in the system were a common issue. A lot of time was spent testing for leaks, usually by evacuating the system and waiting to see if the pressure increased. Sometimes liquid leak detector was used after putting the system, but not the chamber, at an overpressure with N₂ gas. The system was taken apart and reassembled countless times. The results from the first spikes were not understood, and several configurations were tested.

The first design was simply the ²²²Rn source connected to an evacuated acrylic chamber filled with acrylic beads. This made the sample even more similar to the DEAP-3600 AV acrylic, since ²²²Rn would have diffused into the acrylic and the ²¹⁰Pb would be uniformly distributed. Beads of PMMA from Fisher Scientific were selected for the 25–75 μm radius, which is less than the diffusion length of radon in acrylic [45]. A 10 μm filter VCR gasket had to be installed after the pump pulled 7 g of beads through the lines. It would take approximately 1 h to degas the beads. At first, when the beads were not pumped out for long enough, the increase in pressure was confused with a leak. Although the inhibitor was not removed and no initiator was added for polymerization, the MMA monomer was added to make the PMMA beads more like acrylic. Lucas cells were not incorporated, and instead, the pressure changes were used to determine the amount of ²²²Rn transferred from the source to the acrylic chamber. See Figure 7.5.

¹Thanks to Art McDonald and Tony Noble for advice on the spike setup and Lucas cell counting.

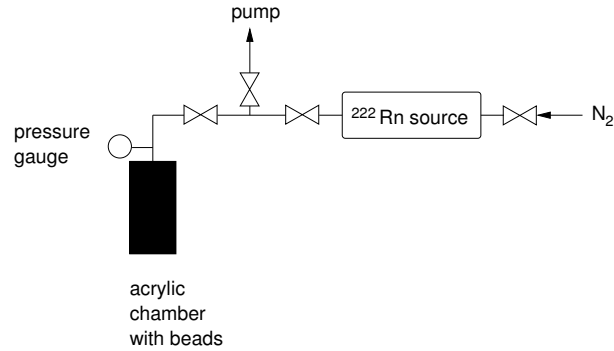


Figure 7.5: The calibrated ^{222}Rn source was opened to an evacuated acrylic chamber filled with PMMA beads. The pressure changes were used to measure the available volumes during free expansion. The acrylic chamber was sealed while ^{222}Rn decayed to ^{210}Pb . Unfortunately, the three spikes prepared with this configuration were not understood.

Using N_2 gas from a cylinder, the source was purged for 1 min and then closed for 1 min to allow mixing. This was repeated five times. The source was left to regenerate for about 10 min. The uncertainty on the time was from closing the valves. The ^{222}Rn activity, A_2 , was calculated from the given equilibrium activity of the source, A_1 , which is the ^{226}Ra activity.

$$A_2 = A_1(1 - e^{-\lambda_2 t}) \quad (7.5)$$

The chamber and the connected tubing were evacuated, which was -30.0 inch Hg on the gauge. The source was opened to the chamber for about 15 s, after which the pressure was -15.5 inch Hg. The acrylic beads occupied some of the volume of the $(170 \pm 20) \text{ cm}^3$ chamber. The mass of the beads was $(100.0 \pm 0.5) \text{ g}$, and the uncertainty was from the electronic scale. From the density of PMMA, 1.2 g/cm^3 [57], the volume of beads was $(83.3 \pm 0.4) \text{ cm}^3$. The available space in the chamber is the difference between the volume of the container and the volume of the beads, $(90 \pm 20) \text{ cm}^3$. The volume of the tubing was found to be $(15 \pm 5) \text{ cm}^3$ by measuring

each component with a ruler. Using the given volume of the source, the unoccupied volume in the chamber was $(40 \pm 10)\%$ of the total volume of the system. The result from the pressure change, $(44 \pm 3)\%$, was used for the calculations. The chamber was sealed for approximately 1 week to allow ^{222}Rn to decay to ^{210}Pb , and then the chamber and line were pumped out for 1 h. The opened chamber was brought to a cleanroom fume hood where 60 mL of monomer was added. This volume of liquid submerged all of the beads. The sample was left to dry in the fume hood. Another acrylic disc was used at the other end to close the chamber. It had a small hole in order to accommodate increased pressure during vaporization.

This setup was used to prepare three spikes. Two blanks were made as well. The blanks were identical to the spikes, but were not exposed to the source. One blank measured (5 ± 2) cpd in the alpha counter. The other blank measured (8 ± 3) cpd in the alpha counter; however, there are two differences to note: a lower temperature of 75°C was used for reducing the volume before ^{210}Po collection, and the 100 mg of ascorbic acid was not measured on a scale with milligram precision.

For the first spike, the source regenerated for 7 min and the ^{222}Rn activity was (475 ± 6) Bq. The pressure change, -11.0 inch Hg, was different than the -15.5 inch Hg in the next two spikes, and the fraction of the gas in the chamber was $(31 \pm 3)\%$ instead of $(44 \pm 3)\%$. The chamber, with (150 ± 10) Bq, was sealed for a week to produce $(5.1 \pm 0.4) \times 10^7$ atoms ^{210}Pb . During the rinse, it was unusual that the two aqua regia rinses practically filled a 30 mL bottle. Typically, a few millilitres were collected from each rinse. That bottle was labelled as Part 1 and the UPW rinse was collected in another bottle, Part 2. Unfortunately, approximately 7 mL of the UPW rinse was spilled. The sample was left for 37 d between rinsing and

^{210}Po collection. The expected (600 ± 50) cpd was halved considering one side of the nickel disc, (300 ± 20) cpd, and halved again for the alphas going toward the detector, (150 ± 10) cpd. After the $(60 \pm 8)\%$ solid angle, (90 ± 10) cpd were expected in the alpha counter. Part 1 of the sample produced 7 counts in 1 d, and Part 2 had no counts in 20 h. About a week later it was noticed that the Alpha 1 detector was covered by a plastic cap, and for how long was unknown. This sample was not used to determine the recovery efficiency.

The source regenerated for 8 min for the second spike. The (540 ± 9) Bq regenerated activity corresponds to (240 ± 20) Bq in the chamber. It was sealed for 6 d to produce $(7.6 \pm 0.5) \times 10^7$ atoms ^{210}Pb . There were 35 d between rinsing and ^{210}Po collection. Considering alphas from one side of the disc and the solid angle, the total expected (840 ± 60) cpd corresponds to (130 ± 20) cpd in the alpha counter. In 25 h of counting, just 9 counts were observed in the ^{210}Po window. It was assumed that the ^{210}Pb remained after ^{210}Po collection, and the effluent was then measured in the well detector. The sample was installed on the well detector 2 weeks later. The amount of ^{210}Pb decay in that time was negligible. The $(7.6 \pm 0.5) \times 10^7$ atoms mean (6500 ± 500) cpd, (280 ± 20) cpd of 46.5 keV gammas, and (150 ± 10) cpd after accounting for the detection efficiency of the well detector. There were 73 counts in 4 d in the ^{210}Pb window, including backgrounds. It should be noted that the monomer was added only 3 d earlier and had not dried completely at the time of vaporization. The lid had been pried off and the sample was sitting open in the warehouse for 1 d. For the vaporization, the lid was sitting with the sample, but was not attached.

A third spike was made to be measured directly in the well detector. To avoid having to wait another week for ^{222}Rn to decay, the source was regenerated for longer,

and the chamber was sealed for only 2 d. After 17 min of regeneration, the ^{222}Rn activity was expected to be (1093 ± 6) Bq which corresponds to (480 ± 30) Bq in the chamber. The amount of ^{210}Pb was $(6.3 \pm 0.4) \times 10^7$ atoms or (5400 ± 400) cpd. The sample was prepared for the well detector. After the branching fraction and the well detector efficiency, (120 ± 10) cpd were expected in the well detector. There were 154 counts in almost 8 d, or (20 ± 2) cpd observed. Similar to the previous spike, this sample had only 3 d for the monomer to dry. No acrylic end was attached to the top of the chamber.

Such low recovery from these three spikes was surprising. There was doubt over the activity of the source, and also how to operate the source. The source may have been damaged but the given calibration of the ^{222}Rn activity, determined at the time of manufacturing, could not be verified. One hypothesis was that the source did not emanate 100% of the produced ^{222}Rn gas, as stated in the manual. There were questions regarding the humidity, and the low pressures. Another explanation was that the available volume in the chamber was incorrect. The beads almost filled the height of the chamber, but by the mass and density, half of the chamber volume was unoccupied. Perhaps, it was only the gap at the top of the chamber that was immediately available for free expansion. Of course, it was possible that vaporization, rinsing, and ^{210}Po collection were ineffective, and that lead volatilized at 500°C , polonium volatilized at 100°C , and that plating of polonium and lead is not understood. More spikes were prepared.

To address whether the source did not function with low pressure, the setup was modified to a flow through configuration. A coil of tubing cooled with LN_2 was used to trap radon. Helium was the carrier gas. A Lucas cell was used to measure the

^{222}Rn , instead of having to make assumptions for a calculation. This setup was similar to that used for the final spike, except that only one Lucas cell was used and that there were beads in the acrylic chamber. The flow through configuration was used for two spike attempts. The first time, helium flowed through the source and cold trap for about 15 min. The trap was evacuated while still in LN_2 , warmed with a heat gun, and opened to the Lucas cell. The Lucas cell was counted right away, and there were 146 counts in 10 min, or 0.2 cps. Due to the low count rate, this run was scrapped before spiking the acrylic chamber. The next time, the source and tubing were purged with helium before adding LN_2 to the tubing. The flow rate was also increased by a factor of four. Again, the Lucas cell measured only 3.6 cps and the run was scrapped.

In case ^{222}Rn was passing the cold trap during helium flow, another configuration was tried. There was no flow, but no vacuum either. The source and trap were purged with helium. The source was closed and isolated, and the trap was closed and isolated. The trap, filled with helium at approximately atmospheric pressure, was cooled with LN_2 . The source was opened to the trap and the ^{222}Rn would have diffused and stopped in the trap. The source was closed. While still in LN_2 , the trap was evacuated for 1 min. The trap was warmed with a heat gun, and then was opened to the Lucas cell for 10 min. Three spikes attempts were made with this setup.

The first had the source opened to the trap for 20 min, after cooling the trap with LN_2 for 10 min. The Lucas cell was counted after 30 min, and during 10 min of counting the rate was 75 cps. For 10 min, the Lucas cell was opened to the evacuated acrylic chamber filled with beads. The Lucas cell was counted again, right away, and 32 cps was measured. Since it seemed that the activity that went to the chamber was

too low, this spike was scrapped.

During the next spike, it was planned to investigate the transfer between two Lucas cells. The trap was cooled for 5 min. The source regenerated for 8 min and then was opened to the trap for 29 min. The Lucas cell was left for an hour before counting. A rate similar to the previous spike was expected; however, the result was more like the background level of the Lucas cell, 0.07 cps. The only reasonable conclusion was that the 2.5 kBq ^{222}Rn generated by the source had leaked from the system. There was no indication of a leak from the pressure gauges during the procedure. After the spike attempt, the system was put at vacuum and only a slight increase was observed in 30 min. The next morning, the system was at atmospheric pressure. A wrench confirmed that all of the fittings were tight. Each piece of copper tubing was examined, and two pieces were found to spin within the fittings. After taking apart the entire system, it was discovered that even tubing pieces that did not move while assembled had loose ferrules. It could have been that the fittings were overtightened and that the brass ferrules cut through the copper tubing, even though the Swagelok instructions had been carefully followed. To make a new connection, the fitting was tightened by hand, tightened 1 and $\frac{1}{4}$ turns with a wrench, removed to inspect the ferrules, tightened by hand and finally tightened $\frac{1}{8}$ turns with a wrench. Thermal expansion after using LN_2 may have affected the brass and copper connections.

The entire system was rebuilt with stainless steel ferrules and tubing before the next spike. The trap was cooled with LN_2 for 5 min. The source was opened to the trap for 25 min. There were 10 min between using the heat gun and opening the trap to the Lucas cell. After 30 min, the Lucas cell measured 1.17 cps over 1 h. This was far too low to spike the acrylic chamber. It was still of interest to transfer between

two Lucas cells. The spiked Lucas cell was opened to the other Lucas cell for 10 min. After 30 min, 1 h of counting revealed 0.72 cps and 0.75 cps. The Lucas cells contained the same amount of ^{222}Rn , as expected, yet the sum was too large. The sum should have been less than the initial amount, and the difference would have indicated the volume of the connecting tubing. The transfer was not understood.

At this point, the idea of using a cold trap at atmospheric pressure was abandoned. It seemed that the most straightforward way to obtain ^{222}Rn from the source was with vacuum. To simplify the volumes, no beads were added to the acrylic chamber. This is the setup that was ultimately used for the successful spike. There were two runs before that. The first was a practice, to understand spiking the Lucas cell, the transfer between two Lucas cells, and the transfer from the Lucas cell to the acrylic chamber. Many of the waiting times and counting times were shortened. For example, the Lucas cells were counted after only 30 min, but for 10 min. The Lucas cells were pumped out for 10 min. The source and trap were purged for 1 min. For 5 min, the trap was evacuated and cooled. The source regenerated for 25 min. The source was opened to the trap for 15 s. There were 10 min allotted for the ^{222}Rn to stop in the trap. The pressure was surprisingly low, < -30 inch Hg. There was no need to evacuate the trap. After using the heat gun, the pressure had increased to -29.0 inch Hg. The trap was opened to the Lucas cell for 10 min. The spiked Lucas cell, which was found to have an activity of 224 cps, was opened to the other Lucas cell for 10 min. There was some increase in pressure but it was off the scale. After, the Lucas cells measured 57 cps and 26 cps. There was a problem with the data files, and Counter A and Counter B seemed to be giving different results. The chamber was pumped out for 5 min. The 57 cps Lucas cell was opened to the chamber. It was then measured to have 36 cps.

It was a relief that the the Lucas cell was finally loaded with a substantial amount of ^{222}Rn , but the transfers were not understood and this spike was scrapped.

The next spike used the same procedure as the successful spike, and a Lucas cell was spiked with (490 ± 60) Bq. The spike was paused overnight. Before transferring between two Lucas cells the following morning, the spiked Lucas cell was counted again. It was expected that the activity would have decreased according to the ^{222}Rn half-life over 18 h. The result was confusing: (610 ± 80) Bq. The procedure continued to the transfer between Lucas cells out of interest. The Lucas cells were counted after 25 h for 10 min, and were (160 ± 20) Bq and (130 ± 20) Bq. The counting was carefully studied with a spiked Lucas cell, before the final spike was made.

I would recommend that another spike be made, to be able to see any variability in the measurement. A blank, or two, would also be interesting. Now that the system is well understood, the acrylic beads should be incorporated. The available volume in the filled chamber could be measured by the pressure change after attaching a Lucas cell at atmospheric pressure. DEAP has 20 kg of beads from RPT that could be used. To be even more like the DEAP-3600 acrylic, the spiked sample could be polymerized. More could be learned about the ^{222}Rn source. It may be possible to verify the ^{222}Rn activity by diluting the gas and using a commercial radon monitor, a RAD7 or a Pylon AB-5, for example. Maybe a germanium detector at Queen's could be used to confirm that there is no ^{226}Ra leaving the source. Studying the Lucas cell spectra for ^{220}Rn could also be pursued.

7.2 Stable lead from Pb standard

The recovery efficiency was also determined using stable lead and inductively coupled plasma mass spectrometry (ICP-MS) performed by an external laboratory. A liquid Pb standard was loaded into acrylic before vaporization. Two pieces of McMaster-Carr acrylic were used. They had been cleaned a year and a half earlier, and were stored in a plastic bag. A machinist drilled a $\frac{3}{8}$ inch hole into the bottom piece, and used a lathe to make a plug on the top piece. The acrylic was cleaned up with Kimwipes and methanol. An electronic balance weighed the 85.7 g bottom piece and 62.1 g top piece. The Pb standard is (1000 ± 4) mg/L Pb in 2% w/w nitric acid. It is prepared with $\text{Pb}(\text{NO}_3)_2$ [94]. A pipette was used to transfer (1.000 ± 0.006) mL into the hole. The uncertainty is the standard deviation for dispensing 1000 μL from the blue, variable volume, Eppendorf Reference pipette [95]. After propagating the uncertainties from the concentration of the Pb standard and the volume from the pipette, the mass of lead was (1.000 ± 0.007) mg. This uncertainty turns out to be negligible. To try to evaporate the liquid, the bottom piece was placed in a small oven at 30°C for 7 h, and later the oven was increased to 40°C for 16 h. There was still liquid in the hole, but we proceeded with vaporization anyway. The mass of the sample, 148.4 g, compared to the mass of the separate pieces, 147.8 g, indicated that there was 0.6 mg of the liquid Pb standard remaining. In the first 15 min of vaporization, the block fell over and slid to the end of the boat. I was concerned that the liquid would spill and vaporize separately from the acrylic, but the pieces stayed together. The pieces did not come apart until after about 40 min, when vaporization was almost complete. With one pass of aqua regia, the yellow-white chalky residue on the boat was removed. The effluent was collected in a 60 mL FEP bottle that was

sent to Testmark Laboratories Ltd. for ICP-MS.

Considering a recovery efficiency of 100%, (1.000 ± 0.007) mg of lead would be collected from the effluent. The lab reports the concentration, and not the mass, of lead. Unfortunately, the total volume of the effluent was not measured. An estimate of (18 ± 2) mL is conservative and is the dominant uncertainty in the calculation of the efficiency. For this spike of stable lead in nitric acid, $(87 \pm 9)\%$ was recovered. See Table 7.4 for the results.

A previous attempt at preparing a spike was abandoned. The idea was to work with a smaller amount of lead. From a pipette, 1 mL of the Pb standard was diluted to 1 L with UPW. Then 1 mL of the 1 ppm solution was pipetted to the bottom acrylic piece and was left to evaporate in the fume hood. By the next day, it had been suggested that perhaps the lead would come out of solution upon being diluted. Concerned that the mass of lead in the acrylic was not known, the liquid was dumped out. The inside of the bottom piece was wiped, and the spike was made with the undiluted Pb standard instead.

In addition to the effluent, two other samples were analysed for lead as an evaluation of the ICP-MS technique. The lab asked that each sample be no less than 20 mL, and that the approximate lead concentration and acid concentration be provided. The Pb standard sample was 20 mL directly from the bottle. Out of curiosity, 50 mL of the diluted Pb standard were sent for analysis. There was no issue with the dilution after all. The lab provides quality control data and demonstrates that a known amount of lead can be measured and that a method blank results in <1 ppb. It would be interesting to analyze an acrylic blank by ICP-MS.

Table 7.4: Stable lead spiked samples analyzed by ICP-MS

Sample	measured ¹ (ppm)	expected (ppm)
Pb standard	956	1000 ± 4
diluted Pb standard	1.030	1.000 ± 0.004
effluent from acrylic vaporization	48.500 ± 0.152	56 ± 6

¹ Uncertainties were not provided, except upon request.

Chapter 8

Results

Acrylic from the DEAP-3600 AV was measured in the well detector and the alpha counter. The recovery efficiency of the spike was first determined, by both the well detector and the alpha counter. To isolate any activity from the acrylic, some blanks were measured in the well detector.

8.1 Blanks

In addition to the empty well detector, an empty PTFE bottle, a PTFE bottle filled with ultrapure acids, a PTFE bottle filled with regular acids, and a PTFE bottle filled with effluent from vaporization and rinsing without acrylic were measured. See Table 8.1. Each PTFE bottle was soaked in aqua regia, from the regular acids, before counting.

In case the regular acids had significant contamination, ultrapure acids were purchased from OPTIMA Fisher Scientific. The certificates of analysis stated <0.01 ppt

uranium and <0.05 ppt thorium. There was <1 ppt and <0.5 ppt lead for the hydrochloric acid and nitric acid, respectively. The blank results show that there is no advantage to using ultrapure acids instead of regular acids.

Two Suprasil boats have been made, referred to as Suprasil 1 and Suprasil 2. The run without acrylic used Suprasil 1, which had been previously used for 15 runs including the spike. The unused Suprasil 2 was selected for rinsing with the ultrapure acids, rinsing with the regular acids, and for the DEAP-3600 AV sample. Before use, Suprasil 2 was rinsed with 50 mL of aqua regia from the ultrapure acids.

Table 8.1: Blanks in the well detector

sample	counts	time (d)	(cpd)
well background	246	23.2	10.6 ± 0.7
bottle	114	12.4	9.2 ± 0.9
ultrapure acids	36	4.3	8.4 ± 1.4
regular acids	22	3.5	6.2 ± 1.3
procedure	42	5.9	7.2 ± 1.1

The lowest background rate should be that of the well detector, since the other blanks are in addition to the rate from the well detector. The fact that the other blanks are lower than the well background may be attributed to attenuation of gammas by the PTFE bottle. The mean and standard deviation of all five blanks, (8.3 ± 1.7) cpd, is taken as the background of a sample in the well detector.

For completeness, the following blanks should be measured in the alpha counter: the sample holder; the nickel disc; ^{210}Po collection; rinsing and ^{210}Po collection; and finally vaporization, rinsing, and ^{210}Po collection.

8.2 Recovery efficiency

The spike was counted in the well detector, and then in the alpha counter. During the rinse, an estimated 3% of effluent was spilled while pouring from Suprasil 1 to the PTFE beaker. In the well detector, there were 110 counts in 3.8 d in the 44.5–48 keV ^{210}Pb window. The signal, (21 ± 3) cpd, is the difference between the sample, (29 ± 3) cpd, and the background, (8.3 ± 1.7) cpd. This is compared to the expected (80 ± 20) cpd. See Figure 8.1.

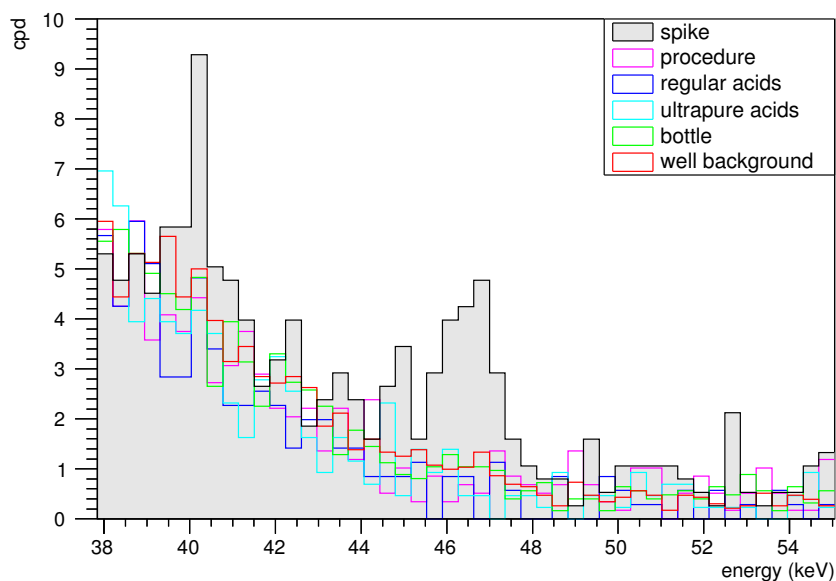


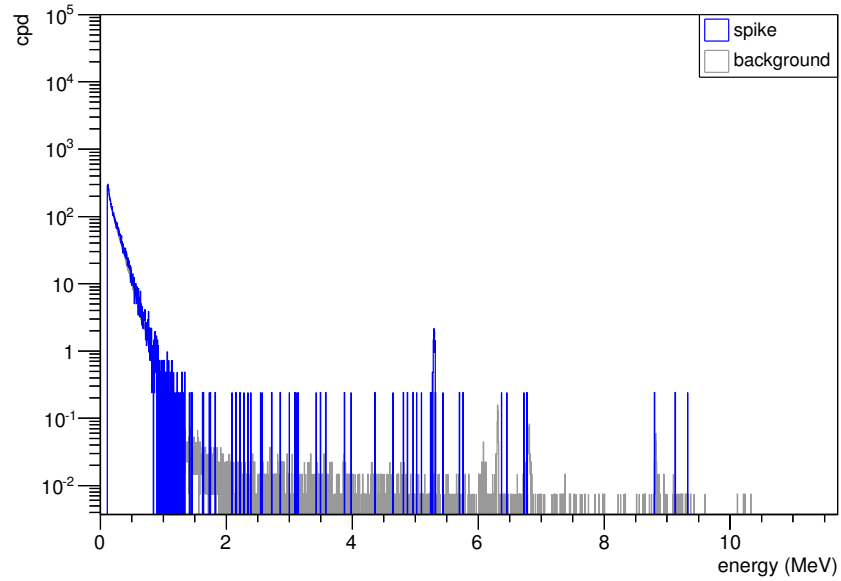
Figure 8.1: The spike was measured in the well detector, and the recovery efficiency was determined to be (26 ± 7) %.

It was difficult to separate the ^{210}Pb signal from other backgrounds in the spike sample. There appeared to be gammas present from the ^{232}Th chain, perhaps from ^{220}Rn . For example, the 39.857 keV gamma from ^{212}Bi is observed [42]. The parent

^{212}Pb is also observed at 238.632 keV. If the sample had been counted for longer, the ^{210}Pb signal would have been better defined.

The spike was then measured in the alpha counter. See Figure 8.2. There were 89 counts in 4 d, or (21 ± 2) cpd, in the 3.5–5.35 keV ^{210}Po window. The background of Alpha 1 was (2.78 ± 0.14) cpd. The signal, (19 ± 2) cpd, was compared to the expected (70 ± 20) cpd.

The peak was fairly well defined at 5.3 MeV and spanned approximately 85 keV. Perhaps the ^{210}Po window should be narrowed from 3.5–5.35 MeV to something like 5.2–5.35 MeV. At 3.5–5.2 keV, the (2.4 ± 0.8) cpd spike sample is consistent with the (2.58 ± 0.14) cpd background. At 5.2–5.35 MeV, the spike sample was (19 ± 2) cpd and the the background was (0.20 ± 0.04) cpd. The recovery efficiency is the same, $(27 \pm 7)\%$, considering the 3.5–5.35 keV window or the 5.2–5.35 keV window.



(a) Full spectrum

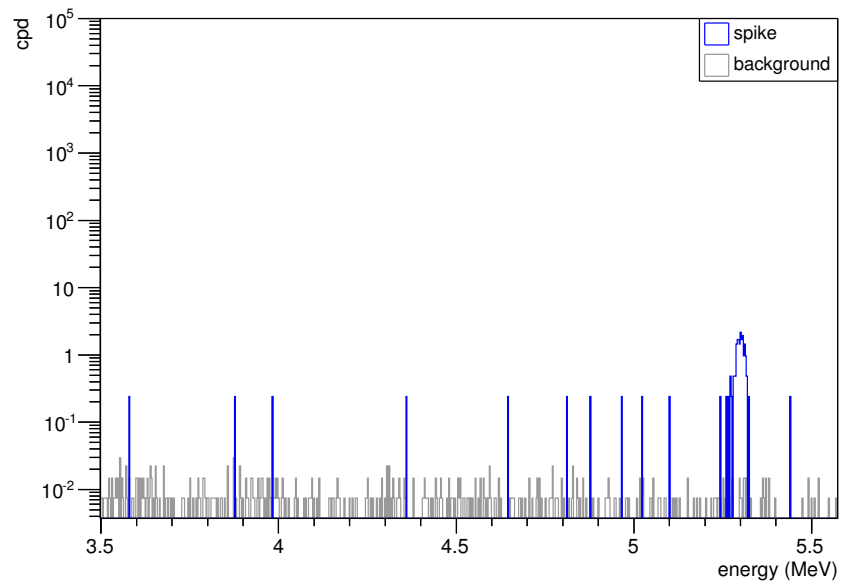
(b) ^{210}Po window

Figure 8.2: The spike was measured in the alpha counter, and the recovery efficiency was determined to be $(27 \pm 7)\%$.

The recovery efficiency from the well detector, $(26 \pm 7) \%$, and from the alpha counter, $(27 \pm 7) \%$, agree. It is conceivable that recovery of the spike was lower than recovery from DEAP-3600 AV acrylic. For example, the different matrix may have caused more volatilization of ^{210}Pb from the spike. Instead of having ^{222}Rn diffuse into acrylic and deposit ^{210}Pb uniformly, the spike would have had ^{210}Pb atoms on the inner walls of the acrylic chamber and only some embedded. In addition, charged ^{222}Rn daughters may have been attracted to the aluminum cap. The recovery efficiency from the spike differs from that measured by ICP-MS of a Pb standard, $(87 \pm 9) \%$. The spike recovery efficiency may be too low, and the stable lead recovery efficiency may be too high. It would be preferable to have the liquid Pb standard dry completely, however, the lead may still be in the form of lead nitrate. Lead is not volatile as a nitrate, but it is as a chloride [48]. Furthermore, it can be argued that the lead behaved differently because it was not incorporated into the acrylic. A better test would be to mix lead with monomer and have that polymerize to form a block of acrylic.

8.3 DEAP-3600 acrylic vessel

An offcut from the DEAP-3600 AV was measured. A 4.0 kg piece, labelled S456DPA-116-01, was first cut to approximately 2 kg on a band saw at Queen's University.¹ The dedicated table saw at SNOLAB was used to make the final dimensions. The outer layer that was removed would have made contact with the band saw, and also would have had more ^{222}Rn from the air. The final sample was 1975.0 g. A boat that had been rinsed with acids, Suprasil 2, was used for the vaporization. Ultrapure acids

¹Thanks to Robert Gagnon. This was just one of many jobs he offered to do in the machine shop.

were used for rinsing. Solid white pieces dissolved upon making contact with aqua regia. The black particles, as usual, did not dissolve. There was some loss in the boat when transferring to the PTFE beaker, although the boat was also sprayed with UPW in an effort to collect all of the residue. Volume reduction took 2.5 h. Again, it was difficult to move the black particles from the PTFE beaker to the 3 mL bottle. The tip of a pipette was cut off to be able to pick up larger pieces.

The DEAP-3600 AV acrylic is consistent with all relevant backgrounds that have been measured. Figure 8.3 shows the well detector results. There were 52 counts in almost 6 d, or (8.9 ± 1.2) cpd. The background of a sample in the well detector is (8.3 ± 1.7) cpd. The signal, (0.6 ± 2.1) cpd, corresponds to (100 ± 400) cpd ^{210}Pb considering the $(26 \pm 7)\%$ recovery efficiency from the well detector, the $(54.4 \pm 0.8)\%$ well detector efficiency at 46.5 keV, and the 4.25% branching fraction. The activity amounts to $(1 \pm 4) \times 10^6$ atoms ^{210}Pb , or $(0.4 \pm 1.4) \times 10^{-15}$ g ^{210}Pb . This gives $(2 \pm 7) \times 10^{-19}$ g/g ^{210}Pb . Using the recovery efficiency measured by ICP-MS of stable lead results in $(0.6 \pm 2.2) \times 10^{-19}$ g/g ^{210}Pb .

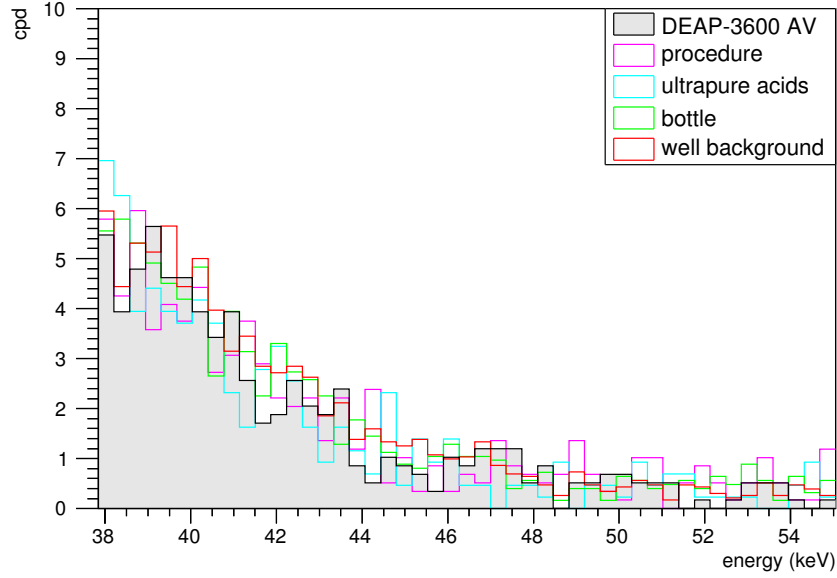
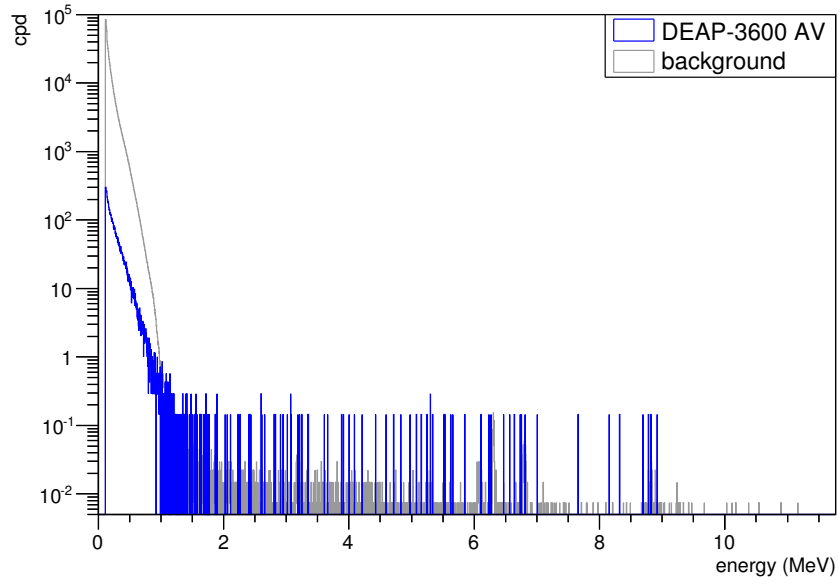


Figure 8.3: From the well detector, the DEAP-3600 AV acrylic has $(2 \pm 7) \times 10^{-19} \text{ g/g } ^{210}\text{Pb}$.

See Figure 8.4 for the alpha counter results. There were 19 counts in 7 d, or (2.7 ± 0.6) cpd at 3.5–5.35 MeV. The background of Alpha 2 was (2.49 ± 0.14) cpd. The signal, (0.3 ± 0.6) cpd, corresponds to (6 ± 16) cpd ^{210}Po considering the $(27 \pm 7)\%$ recovery efficiency and the $(15 \pm 2)\%$ counting efficiency. The effluent was left for 41 d. The ^{210}Po activity amounts to $(0.5 \pm 1.2) \times 10^6$ atoms ^{210}Pb , or $(1.6 \pm 4.1) \times 10^{-16} \text{ g } ^{210}\text{Pb}$, which corresponds to $(0.8 \pm 2.1) \times 10^{-19} \text{ g/g } ^{210}\text{Pb}$.

In the narrow 5.2–5.35 MeV window, there were 4 counts which corresponds to $(1.2 \pm 1.0) \times 10^{-19} \text{ g/g } ^{210}\text{Pb}$.



(a) Full spectrum

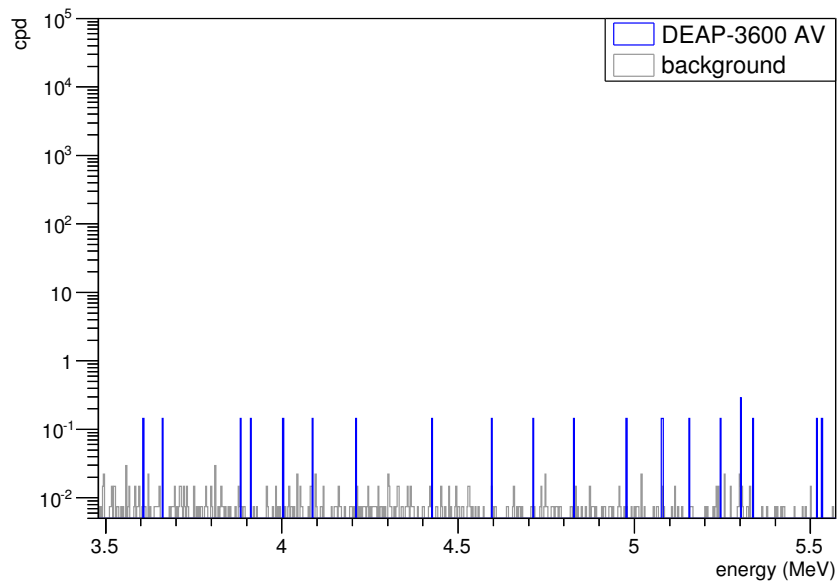
(b) ^{210}Po window

Figure 8.4: From the alpha counter, the DEAP-3600 AV acrylic has $(0.8 \pm 2.1) \times 10^{-19} \text{ g/g } ^{210}\text{Pb}$.

The sample from the DEAP-3600 AV was at the level of 10^{-19} g/g ^{210}Pb . Recall that the maximum tolerable concentration is 1.1×10^{-20} g/g ^{210}Pb . The sample was consistent with background in both the well detector and alpha counter, therefore the measurement may be improved by increasing the count rate with a larger quantity of acrylic. There are nine pieces, 63.0 kg, of offcuts from the DEAP-3600 AV, as well as a 200 kg spare gore and 60 kg of a broken gore. A 10 kg sample, from five 2 kg blocks, is recommended. In any event, the procedure should be repeated to demonstrate reproducibility.

Chapter 9

Conclusion

During the search for dark matter with DEAP-3600, understanding the radiopurity of detector materials is crucial. Such a rare signal drives the tolerable background to extremely low levels. The AV has a limit of 1.1×10^{-20} g/g ^{210}Pb . An acrylic assay that is based on vaporization has been developed. A large quantity of acrylic was vaporized and the residue was collected by rinsing with heated aqua regia. The concentrated sample was counted in an ultralow background HPGe well detector. The sample was stored to allow ^{210}Pb to decay to ^{210}Po . Then the ^{210}Po was deposited on discs and measured in a low background alpha counter. A ^{210}Pb spike was made from a ^{222}Rn source. The spike recovery efficiency was measured to be $(26 \pm 7)\%$ by the well detector, and $(27 \pm 7)\%$ by the alpha counter. This was compared to the $(87 \pm 9)\%$ recovery efficiency of stable lead from a Pb standard that was measured by ICP-MS. A 2 kg offcut from the DEAP-3600 AV was measured. From the well detector, the result was $(2 \pm 7) \times 10^{-19}$ g/g ^{210}Pb considering the spike recovery efficiency. If the ICP-MS recovery efficiency is used instead, the result becomes $(0.6 \pm 2.2) \times 10^{-19}$ g/g ^{210}Pb . From the alpha counter, and a 3.5–5.35 MeV ^{210}Po

window, the result was $(0.8 \pm 2.1) \times 10^{-19}$ g/g ^{210}Pb . With a smaller ^{210}Po window of 5.2–5.35 MeV, the result becomes $(1.2 \pm 1.0) \times 10^{-19}$ g/g. Overall, all of the calculated results are consistent and at the level of 10^{-19} g/g ^{210}Pb . This is the most sensitive limit on ^{210}Pb in acrylic to date.

Bibliography

- [1] F. Zwicky, “Die Rotverschiebung von extragalaktischen Nebeln,” *Helv. Phys. Acta*, vol. 6, pp. 110–127, 1933.
- [2] F. Zwicky, A. Krasinski (Ed.), “Republication of: The redshift of extragalactic nebulae,” *Gen. Relat. Gravit.*, vol. 41, pp. 207–224, 2009.
- [3] V. C. Rubin and W. K. Ford, Jr., “Rotation of the Andromeda Nebula from a spectroscopic survey of emission regions,” *Astrophys. J.*, vol. 159, pp. 379–403, 1970.
- [4] D. Clowe, A. Gonzalez, and M. Markevitch, “Weak-lensing mass reconstruction of the interacting cluster 1E 0657-558: Direct evidence for the existence of dark matter,” *Astrophys. J.*, vol. 604, pp. 596–603, 2004.
- [5] P. A. R. Ade *et al.* (Planck Collaboration), “Planck 2013 results. XVI. Cosmological parameters.” arXiv:1303.5076.
- [6] R. Bernabei *et al.*, “New results from DAMA/LIBRA,” *Eur. Phys. J. C*, vol. 67, pp. 39–49, 2010.
- [7] J. Amaré *et al.*, “Update on the ANAIS experiment. ANAIS-0 prototype results at the new Canfranc Underground Laboratory,” *12th International Conference*

- on Topics in Astroparticle and Underground Physics (TAUP 2011)*. *J. Phys. Conf. Ser.*, vol. 375, p. 012026, 2012.
- [8] J. Cherwinka *et al.*, “A search for the dark matter annual modulation in South Pole ice,” *Astropart. Phys.*, vol. 35, pp. 749–754, 2012.
- [9] H. S. Lee *et al.* (KIMS Collaboration), “Limits on interactions between weakly interacting massive particles and nucleons obtained with CsI(Tl) crystal detectors,” *Phys. Rev. Lett.*, vol. 99, p. 091301, 2007.
- [10] Z. Ahmed *et al.* (The CDMS II Collaboration), “Dark matter search results from the CDMS II experiment,” *Science*, vol. 327, pp. 1619–1621, 2010.
- [11] Z. Ahmed *et al.* (CDMS Collaboration), “Results from a low-energy analysis of the CDMS II germanium data,” *Phys. Rev. Lett.*, vol. 106, p. 131302, 2011.
- [12] R. Agnese *et al.* (CDMS Collaboration), “Silicon detector dark matter results from the final exposure of CDMS II.” arXiv:1304.4279.
- [13] E. Armengaud *et al.* (EDELWEISS Collaboration), “Final results of the EDELWEISS-II WIMP search using a 4-kg array of cryogenic germanium detectors with interleaved electrodes,” *Phys. Lett. B*, vol. 702, pp. 329–335, 2011.
- [14] G. Angloher *et al.*, “Results from 730 kg days of the CRESST-II Dark Matter search,” *Eur. Phys. J. C*, vol. 72, p. 1971, 2012.
- [15] C. E. Aalseth *et al.* (CoGeNT Collaboration), “CoGeNT: A search for low-mass dark matter using p -type point contact germanium detectors,” *Phys. Rev. D*, vol. 88, p. 012002, 2013.

- [16] J. Monroe, “Recent progress from the MiniCLEAN dark matter experiment,” *12th International Conference on Topics in Astroparticle and Underground Physics (TAUP 2011)*. *J. Phys. Conf. Ser.*, vol. 375, p. 012012, 2012.
- [17] J. Liu (XMASS Collaboration), “The XMASS 800 kg detector,” *12th International Conference on Topics in Astroparticle and Underground Physics (TAUP 2011)*. *J. Phys. Conf. Ser.*, vol. 375, p. 012022, 2012.
- [18] D. S. Akerib *et al.*, “First results from the LUX dark matter experiment at the Sandford Underground Research Facility.” arXiv:1310.8214.
- [19] D. Akimov *et al.*, “WIMP-nucleon cross-section results from the second science run of ZEPLIN-III,” *Phys. Lett. B*, vol. 709, pp. 14–20, 2012.
- [20] E. Aprile *et al.* (XENON100 Collaboration), “Dark matter results from 225 live days of XENON100 data,” *Phys. Rev. Lett.*, vol. 109, p. 181301, 2012.
- [21] C. Regenfus (ArDM Collaboration), “The argon dark matter experiment (ArDM),” *Topics in Astroparticle and Underground Physics (TAUP 2009)*. *J. Phys. Conf. Ser.*, vol. 203, p. 012024, 2010.
- [22] P. Benetti *et al.* (WARP Collaboration), “First results from a dark matter search with liquid argon at 87 K in the Gran Sasso underground laboratory,” *Astropart. Phys.*, vol. 28, pp. 495–507, 2008.
- [23] D. Akimov *et al.* (DarkSide Collaboration), “Light yield in DarkSide-10: A prototype two-phase liquid argon TPC for dark matter searches.” arXiv:1204.6218.
- [24] S. Archambault *et al.*, “Constraints on low-mass WIMP interactions on ^{19}F from PICASSO,” *Phys. Lett. B*, vol. 711, pp. 153–161, 2012.

- [25] E. Behnke *et al.* (COUPP Collaboration), “First dark matter search results from a 4-kg CF₃ bubble chamber operated in a deep underground site,” *Phys. Rev. D*, vol. 86, p. 052001, 2012.
- [26] M. Felizardo *et al.* (The SIMPLE Collaboration), “Final analysis and results of the Phase II SIMPLE dark matter search,” *Phys. Rev. Lett.*, vol. 108, p. 201302, 2012.
- [27] M. Pipe (DRIFT Collaboration), “Background reduction and spin-dependent limits using DRIFT - a directionally sensitive dark matter detector,” *VI International Workshop on the Dark side of the Universe (DSU 2010)*. *J. Phys. Conf. Ser.*, vol. 315, p. 012017, 2011.
- [28] S. Ahlen *et al.* (DMTPC Collaboration), “First dark matter search results from a surface run of the 10-L DMTPC directional dark matter detector,” *Phys. Lett. B*, vol. 695, pp. 124–129, 2011.
- [29] J. Billard, F. Mayet, and D. Santos, “Directional detection of dark matter with MIMAC,” *12th International Conference on Topics in Astroparticle and Underground Physics (TAUP 2011)*. *J. Phys. Conf. Ser.*, vol. 375, p. 012008, 2012.
- [30] J. Barreto *et al.*, “Direct search for low mass dark matter particles with CCDs,” *Phys. Lett. B*, vol. 711, pp. 264–269, 2012.
- [31] Gaitskell, Mandic, and Filippini. <http://dmtools.brown.edu> Retrieved 18 November 2013.

- [32] M. G. Boulay and A. Hime, “Technique for direct detection of weakly interacting massive particles using scintillation time discrimination in liquid argon,” *Astropart. Phys.*, vol. 25, pp. 179–182, 2006.
- [33] A. Hitachi, T. Takahashi, N. Funayama, K. Masuda, J. Kikuchi, and T. Doke, “Effect of ionization density on the time dependence of luminescence from liquid argon and xenon,” *Phys. Rev. B*, vol. 27, no. 9, pp. 5279–5285, 1983.
- [34] M. G. Boulay *et al.*, “Measurement of the scintillation time spectra and pulse-shape discrimination of low-energy β and nuclear recoils in liquid argon with DEAP-1.” arXiv:0904.2930.
- [35] P.-A. Amaudruz *et al.*, “Radon backgrounds in the DEAP-1 liquid argon based Dark Matter detector.” arXiv:1211.0909.
- [36] M. G. Boulay (DEAP Collaboration), “DEAP-3600 dark matter search at SNOLAB,” *12th International Conference on Topics in Astroparticle and Underground Physics (TAUP 2011)*. *J. Phys. Conf. Ser.*, vol. 375, p. 012027, 2012.
- [37] A. McDonald, “Depleted argon.” DEAP Collaboration meeting, April 2013.
- [38] B. Cai, M. Boulay, M. Kuźniak, and P. Skensved, “Neutron backgrounds in DEAP-3600.” DEAP STR-2011-009 Rev 2, 2011.
- [39] B. Cai, M. Batygov, M. Boulay, B. Cleveland, S. Florian, C. Jillings, M. Kuźniak, T. Pollmann, and W. Rau (DEAP Collaboration), “Surface background control in DEAP-3600.” DEAP STR-2010-011 v6, 2010.

- [40] B. Cai, M. Boulay, B. Cleveland, and T. Pollmann (DEAP Collaboration), “Surface backgrounds in the DEAP-3600 dark matter experiment,” *Topical Workshop on Low Radioactivity Techniques – LRT 2010. AIP Conf. Proc.*, vol. 1338, pp. 137–146, 2011.
- [41] T. Pollmann, M. Boulay, and M. Kuźniak, “Scintillation of thin tetraphenyl butadiene films under alpha particle excitation,” *Nucl. Instrum. Meth. A*, vol. 635, pp. 127–130, 2011.
- [42] National Nuclear Data Center, “NuDat 2 database.” <http://www.nndc.bnl.gov/nudat2>, 2013.
- [43] M. J. Berger, J. S. Coursey, M. A. Zucker, and J. Chang, “ESTAR, PSTAR, and ASTAR: Computer programs for calculating stopping-power and range tables for electrons, protons, and helium ions (version 1.2.3).” National Institute of Standards and Technology, <http://physics.nist.gov/Star>, Retrieved 17 August 2013, 2005.
- [44] M. Kuźniak, M. G. Boulay, and T. Pollmann, “Surface roughness interpretation of 730 kg days CRESST-II results,” *Astropart. Phys.*, vol. 36, pp. 77–82, 2012.
- [45] M. Wojcik, “Measurement of radon diffusion and solubility constants in membranes,” *Nucl. Instrum. Meth. B*, vol. 61, pp. 8–11, 1991.
- [46] M. Boulay, “Radon diffusion and acrylic background requirements for DEAP-3600.” DEAP STR-2009-006, 2009.

- [47] C. Jillings (DEAP Collaboration), “Control of contamination of radon-daughters in the DEAP-3600 acrylic vessel,” *Low Radioactivity Techniques 2013 (LRT 2013) AIP Conf. Proc.*, vol. 1549, pp. 86–89, 2013.
- [48] T. T. Gorsuch, “Radiochemical investigations on the recovery for analysis of trace elements in organic and biological materials,” *Analyst*, vol. 84, pp. 135–173, 1959.
- [49] Y. Y. Ebaid and A. E. M. Khater, “Determination of ^{210}Pb in environmental samples,” *J. Radioanal. Nucl. Chem.*, vol. 270, no. 3, pp. 609–619, 2006.
- [50] D. Larivière, K. M. Reiber, R. D. Evans, and R. J. Cornett, “Determination of ^{210}Pb at ultra-trace levels in water by ICP-MS,” *Anal. Chim. Acta*, vol. 549, pp. 188–196, 2005.
- [51] B. Cleveland and I. Lawson, “SNOLAB gamma assay facility.” <https://www.snolab.ca/users/services/gamma-assay/index.html>, Updated 26 November 2013.
- [52] A. Martin and R. L. Blanchard, “The thermal volatilisation of caesium-137, polonium-210 and lead-210 from *in vivo* labelled samples,” *Analyst*, vol. 94, pp. 441–446, 1969.
- [53] R. L. Blanchard, “Rapid determination of lead-210 and polonium-210 in environmental samples by deposition on nickel,” *Anal. Chem.*, vol. 38, no. 2, pp. 189–192, 1966.
- [54] C. D. Biggin, G. T. Cook, A. B. MacKenzie, and J. M. Pates, “Time-efficient method for the determination of ^{210}Pb , ^{210}Bi , and ^{210}Po activities in seawater

- using liquid scintillation spectrometry,” *Anal. Chem.*, vol. 74, no. 3, pp. 671–677, 2002.
- [55] M. Wadorski, “Low level ^{210}Pb measurements using beta/gamma coincidence.” DEAP Collaboration meeting, April 2013.
- [56] C. M. Nantais, B. T. Cleveland, and M. G. Boulay, “Radiopurity measurement of acrylic for DEAP-3600,” *Low Radioactivity Techniques 2013 (LRT 2013) AIP Conf. Proc.*, vol. 1549, pp. 185–188, 2013.
- [57] W. M. Haynes (Ed.), *CRC handbook of chemistry and physics, 93rd edition*. Boca Raton, FL: CRC Press/Taylor and Francis, Internet Version 2013.
- [58] Matheson Tri-Gas, Inc. MSDS, “Methyl methacrylate, inhibited.” <http://www.chemadvisor.com/Matheson/database/msds/mat14630000800003.pdf>, Retrieved 01 July 2013, 2013.
- [59] Ontario Ministry of Labour, “Current occupational exposure limits for Ontario workplaces required under Regulation 833.” http://www.labour.gov.on.ca/english/hs/pubs/oe1_table.php Retrieved 01 July 2013, 2013.
- [60] R. N. Ghosh, I. S. Wichman, C. A. Kramer, and R. Loloee, “Time-resolved measurements of pyrolysis and combustion products of PMMA,” *Fire Mater.*, vol. 37, pp. 280–296, 2013.
- [61] P. J. Linstrom and W. G. Mallard (Eds.), “NIST Chemistry WebBook.” NIST Standard Reference Database Number 69, National Institute of Standards and Technology, <http://webbook.nist.gov>, Retrieved 03 June 2013, 2011.

- [62] B. J. Holland and J. N. Hay, "The kinetics and mechanisms of the thermal degradation of poly(methyl methacrylate) studied by thermal analysis-Fourier transform infrared spectroscopy," *Polymer*, vol. 42, pp. 4825–4835, 2001.
- [63] B. J. Holland and J. N. Hay, "The effect of polymerisation conditions on the kinetics and mechanisms of thermal degradation of PMMA," *Polym. Degrad. Stabil.*, vol. 77, pp. 435–439, 2002.
- [64] S. Ozlem, E. Aslan-Gürel, R. M. Rossi, and J. Hacaloglu, "Thermal degradation of poly(isobornyl acrylate) and its copolymer with poly(methyl methacrylate) via pyrolysis mass spectrometry," *J. Anal. Appl. Pyrol.*, vol. 100, pp. 17–25, 2013.
- [65] M. Newborough, D. Highgate, and P. Vaughan, "Thermal depolymerisation of scrap polymers," *Appl. Therm. Eng.*, vol. 22, pp. 1875–1883, 2002.
- [66] O. Li, "Acrylic vaporization system flowsheet." SLDO-DEC-FL-7702-01 Rev 1, 2011.
- [67] C. Nantais, "Vaporization procedure for the acrylic assay." SLDO-DEC-MN-7706-00 Rev 4, 2012.
- [68] B. Cleveland, F. Duncan, and C. Nantais, "Acrylic vaporization system hazard assessment." SLDO-DEC-TR-0021 Rev 0, 2011.
- [69] G. M. Milton, S. J. Kramer, R. J. E. Deal, and E. D. Earle, "Ultra trace analysis of acrylic for ^{232}Th and ^{238}U daughters," *Appl. Radiat. Isot.*, vol. 45, no. 5, pp. 539–547, 1994.

- [70] C. Nantais, “Chemistry procedure for the acrylic assay.” SLDO-DEC-MN-7706-02 Rev D, 2012.
- [71] Cole-Parmer, “Chemical compatibility database.” <http://www.coleparmer.ca/Chemical-Resistance>, Retrieved 26 August 2013, 2013.
- [72] C. Cazala, J. L. Reyss, J. L. Decossas, and A. Royer, “Improvement in the determination of ^{238}U , $^{228-234}\text{Th}$, $^{226-228}\text{Ra}$, ^{210}Pb , and ^7Be by γ spectrometry on evaporated fresh water samples,” *Environ. Sci. Technol.*, vol. 37, no. 21, pp. 4990–4993, 2003.
- [73] I. Lawson and B. Cleveland, “Low background counting techniques at SNOLAB,” *Low Radioactivity Techniques 2013 (LRT 2013) AIP Conf. Proc.*, vol. 1549, pp. 16–19, 2013.
- [74] I. T. Lawson, “Radon levels in the SNOLAB underground laboratory.” http://www.snolab.ca/users/library/technotes/lawson/radon_underground.pdf, July 2013.
- [75] I. T. Lawson, “Radon concentration levels in various surface locations,” February 2010.
- [76] M. Wójcik and G. Zuzel, “Low- ^{222}Rn nitrogen gas generator for ultra-low background counting systems,” *Nucl. Instrum. Meth. A*, vol. 539, pp. 427–432, 2005.
- [77] B. T. Cleveland and I. T. Lawson, “Measurement of the counting efficiency of the SNOLAB Ge well detector,” March 2013.

- [78] Canberra data sheet, “Germanium Well detector (WELL).” <http://www.canberra.com/products/detectors/germanium-detectors.asp>, Retrieved 05 August 2013, 2012.
- [79] T. Pilleyre, S. Sanzelle, D. Miallier, J. Faïn, and F. Courtine, “Theoretical and experimental estimation of self-attenuation corrections in determination of ^{210}Pb by γ -spectroscopy with well Ge detector,” *Radiat. Meas.*, vol. 41, pp. 323–329, 2006.
- [80] K. M. Matthews, C.-K. Kim, and P. Martin, “Determination of ^{210}Po in environmental materials: A review of analytical methodology,” *Appl. Radiat. Isot.*, vol. 65, pp. 267–279, 2007.
- [81] I. M. Fisenne, “Polonium.” Environmental Measurements Laboratory Procedure Manual, 28th edition. Volume I, U.S. Department of Energy Report HASL-300 Rev. 0, February 1997.
- [82] E. Ansoborlo, P. Berard, C. Den Auwer, R. Leggett, F. Menetrier, A. Younes, G. Montavon, and P. Moisy, “Review of chemical and radiotoxicological properties of polonium for internal contamination purposes,” *Chem. Res. Toxicol.*, vol. 25, pp. 1551–1564, 2012.
- [83] J. J. Cleary and E. I. Hamilton, “Loss of polonium-210 on dry ashing rat tissues in a muffle furnace,” *Analyst*, vol. 93, pp. 235–236, 1968.
- [84] R. W. Helmkamp, W. F. Bale, and V. Hrynyszyn, “The determination of ^{210}Po and ^{210}Bi in human urine by direct extraction on nickel,” *Int. J. Appl. Radiat. Isot.*, vol. 30, pp. 237–246, 1979.

- [85] F. Henricsson, Y. Ranebo, E. Holm, and P. Roos, “Aspects on the analysis of ^{210}Po ,” *J. Environ. Radioact.*, vol. 102, pp. 415–419, 2011.
- [86] S. C. Ehinger, R. A. Pacer, and F. L. Romines, “Separation of the radioelements $^{210}\text{Pb} - ^{210}\text{Bi} - ^{210}\text{Po}$ by spontaneous deposition onto noble metals and verification by Cherenkov and liquid scintillation counting,” *J. Radioanal. Nucl. Chem. Art.*, vol. 98, no. 1, pp. 39–48, 1986.
- [87] C.-K. Kim, M. H. Lee, and P. Martin, “Method validation of a procedure for determination of ^{210}Po in water using DDTC solvent extraction and Sr resin,” *J. Radioanal. Nucl. Chem.*, vol. 279, no. 2, pp. 639–646, 2009.
- [88] ORTEC data sheet, “ULTRA and ULTRA AS: Ion-implanted-silicon charged-particle detectors.” <http://www.ortec-online.com/Solutions/alpha-spectroscopy.aspx> Retrieved 10 July 2013, 2012.
- [89] Pylon Electronics Inc., “Pylon model RN-1025 flow through radon gas source.” Instruction Manual, A900030 Rev 3, 2001.
- [90] K. S. Krane, *Introductory nuclear physics, 3rd edition*. New York: Wiley, 1987.
- [91] I. Blevis *et al.*, “Measurement of ^{222}Rn dissolved in water at the Sudbury Neutrino Observatory,” *Nucl. Instrum. Meth. A*, vol. 517, pp. 139–153, 2004.
- [92] M. Liu, H. W. Lee, and A. B. McDonald, “ ^{222}Rn emanation into vacuum,” *Nucl. Instrum. Meth. A*, vol. 329, pp. 291–298, 1993.
- [93] M. Liu, “ ^{222}Rn emanation into vacuum,” Master’s thesis, Queen’s University, (1991).

- [94] Sigma-Aldrich Co. LLC., “16595 FLUKA Lead standard for AAS: TraceCERT, 1000 mg/L Pb in nitric acid.” <http://www.sigmaaldrich.com/catalog/product/fluka/16595?lang=en®ion=CA>, Retrieved 11 July 2013, 2013.
- [95] Eppendorf brochure, “Eppendorf Reference: The pipette.” http://eshop.eppendorf.ca/products/Eppendorf_Reference_adjustable-volume_pipettes, Retrieved 28 June 2013, 2010.